ANALYSES OF WOLVERINE DNA MARK-RECAPTURE SAMPLING IN THE NORTHWEST TERRITORIES 2004-2015

MURRAY EFFORD [1], JOHN BOULANGER [2], ROBERT MULDERS [3]

[1] DUNEDIN, NEW ZEALAND, [2] INTEGRATED ECOLOGICAL RESEARCH, NELSON, BC, [3] YELLOWKNIFE, NT

2024

MANUSCRIPT NUMBER 314

ABSTRACT

The population of wolverines at five sites in the Northwest Territories (Daring Lake, Diavik, Ekati, Gahcho Kué and Snap Lake) were surveyed intermittently over 2004–2015. Wolverines were identified individually from DNA in hairs left at baited posts spaced 3-5 km apart. Spatially explicit capture–recapture methods were used to estimate population density and overcome the confounding of population trend with changes in area sampled at three sites. Trend estimates were also obtained from non-spatial open-population capture–recapture analyses. Simulation was used to assess the power of various sampling designs to detect trend.

The main results were:

- The trapping areas of the three adjoining northern grids (Daring Lake, Diavik and Ekati) overlapped because of the large home ranges of wolverines. It was therefore not possible to separate the population into components associated with single grids.
- The Daring Lake site was sampled intensively, starting a year before the other grids. Data from Daring Lake taken alone indicated a decline in wolverine density. Spatial capture–recapture estimates of population trend from each of the other sites separately also suggested overall decline in the decade 2005–2014, but 95% confidence intervals overlapped 1.0 (no change).
- We combined data from the northern sites (Daring Lake, Diavik and Ekati) for a robust estimate of overall trend in the region. Average density declined by about 40% between 2005 and 2014, from 5.57 per 1,000 km^2 to 3.32 per 1,000 km^2.
- Sex ratio was even or female biased.
- We make suggestions regarding future wolverine sampling that largely echo previous recommendations (Boulanger and Mulders 2013b) each sampling grid should be as large as logistically feasible (because precision is increased when more wolverines are sampled).
- By spacing posts 5 km apart over a modestly increased sampling area it is possible to improve the power of the design to detect change in wolverine density while potentially reducing costs
- Over the long term, population trend may be measured adequately with less frequent (four to six yearly) sampling. However, we do not recommend longer intervals because precision is then reduced for estimates of survival and recruitment, and it will be years before any change in trend is recognised.
- From a conservation perspective, the potential change in population size between samples should be considered when determining sampling interval. For example, at the current rate of decline (6% per year) the population would be reduced by 27% in five years.
- Sampling should be synchronous across sites (all sites should be sampled in one year to allow data to be combined for analysis).
- Protocols for post placement, sample collection and laboratory processing should be applied consistently across sites.

- All sites should use a common electronic data format. Ideally there would be a single database; in lieu of that, spreadsheets should use precisely the same column names in the same order and with the same data types.

TABLE OF CONTENTS

LIST OF FIGURES

LIST OF TABLES

INTRODUCTION

Wolverines (*Gulo gulo*) are distributed widely across the Canadian low Arctic, but their populations are sparse, potentially threatened by novel human impacts, and difficult to survey. Mulders et al. (2007) established a capture–recapture methodology for surveying wolverines that used DNA from baited hair snags (posts) and applied it in 2004 over four ten-day sampling sessions at Daring Lake in the Northwest Territories (NWT). Slightly less intensive hair-snag sampling, with two ten-day sessions per year, was performed at Daring Lake and at four other sites intermittently from 2005–2015, for a total of 24 site x year datasets. Subsets of the present data were analyzed by Boulanger and Mulders (2013a,b). We report capture–recapture analyses of all datasets with the aim of assessing spatial and temporal variation in wolverine density.

Our statistical analysis used a number of advanced capture–recapture methods. The main tool was spatially explicit capture–recapture (SECR), an extension of conventional capture–recapture methods specifically for estimating the density of spatially distributed populations using passive sampling devices (Efford 2004, Borchers and Efford 2008, Royle et al. 2014). SECR avoids most of the concerns about geographic closure that featured in earlier analyses using conventional closed-population methods (e.g. Mulders et al. 2007). SECR is described more fully in Appendix 2.

The design pioneered at Daring Lake has proved highly effective for sampling wolverine populations. However, the cost of each survey is considerable, and it is reasonable to ask whether estimates with similar or greater precision could be obtained for less cost. We therefore assessed the consequences of varying the spacing of posts and frequency of sampling and make suggestions regarding future sampling.

This analysis was done in 2018; since then, there has been much relevant research on SECR and wolverines that is not cited here (e.g. Efford and Boulanger 2019, Efford and Schofield 2020, Barrueto et al. 2022, Milleret et al. 2022). We recommend readers review these papers for an updated discussion on some of the topics covered in this report.

METHODS

Field and Laboratory Methods

Sampling was conducted at five sites (latitude 63°–65°N, longitude 108°–112°W) between 2004 and 2015. The study areas were in the Taiga shield with southern grids on the edge of treeline (Figure 1).

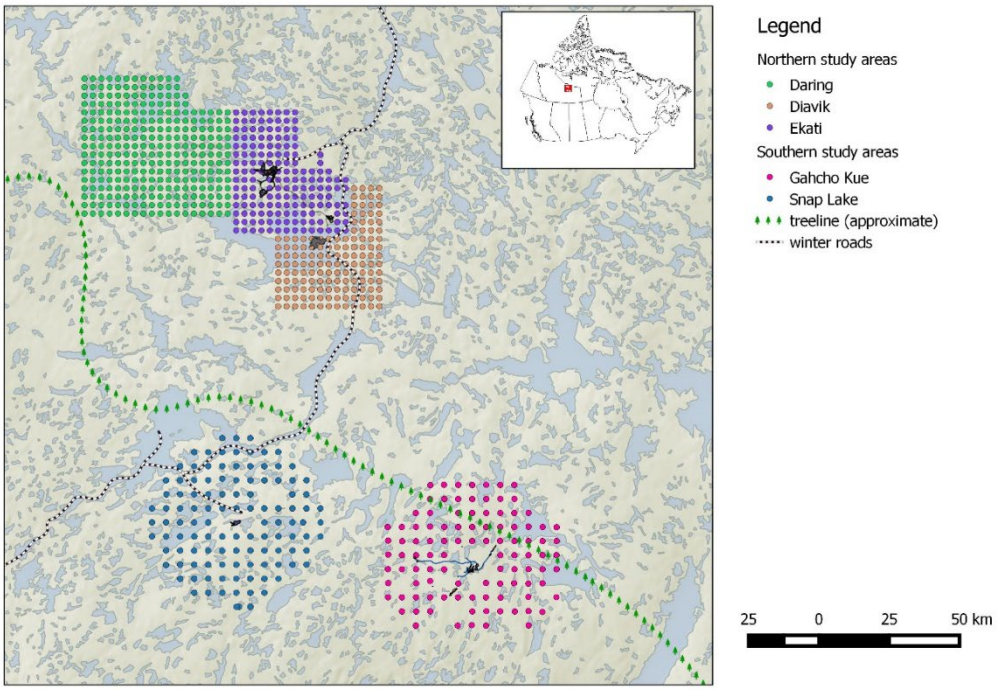

Figure 1. Wolverine study areas in the NWT. Dots indicate the locations of posts for DNA sampling in 2014 or 2015 (Ekati only). Nominal footprints of the mines are displayed.

Not all sites were sampled in the same year (Table 1, Figure 2). Sampling at each site used a grid of baited posts (Figures 1, 2). Posts were placed on a square grid approximately 3 km apart except for Snap Lake and Gahcho Kué in 2013 and 2014, when the spacing was 5 km. In 2004, the grid at Daring Lake was moved 1.5 km east, south, and west between successive sessions; the effect was to sample points on a 1.5 km grid for one session each. Overall, the data comprised 24 site x year samples (Table 1).

Table 1. Number of posts used in wolverine surveys at five sites over 2004–2015. There was no sampling in 2008 or 2012. Posts were spaced 3 km apart except for Gahcho Kué and Snap Lake in 2013–2014 (5 km). Sampling was for two consecutive periods in April and early May of about ten days each, except for DA in 2004 when sampling was over four ten-day periods (22 March – 9 May) and posts were moved 1.5 km between samples (Mulders et al. 2007).

Site		**Year**											
		2004	2005	2006	2007	2008	2009	2010	2011	2012	2013	2014	2015
Daring Lake	DA	284	284	284	284	.	284	.	275	.	284	284	.
Diavik	DI	.	141	141	.	.	.	134	134	.	.	134	.
Ekati	EK	.	118	132	.	.	.	183	116	.	.	.	184
Gahcho Kué	GK	.	175	175	.	.	.	.	.	.	68	79	.
Snap Lake	SL	.	.	.	.	.	.	.	.	.	55	113	.

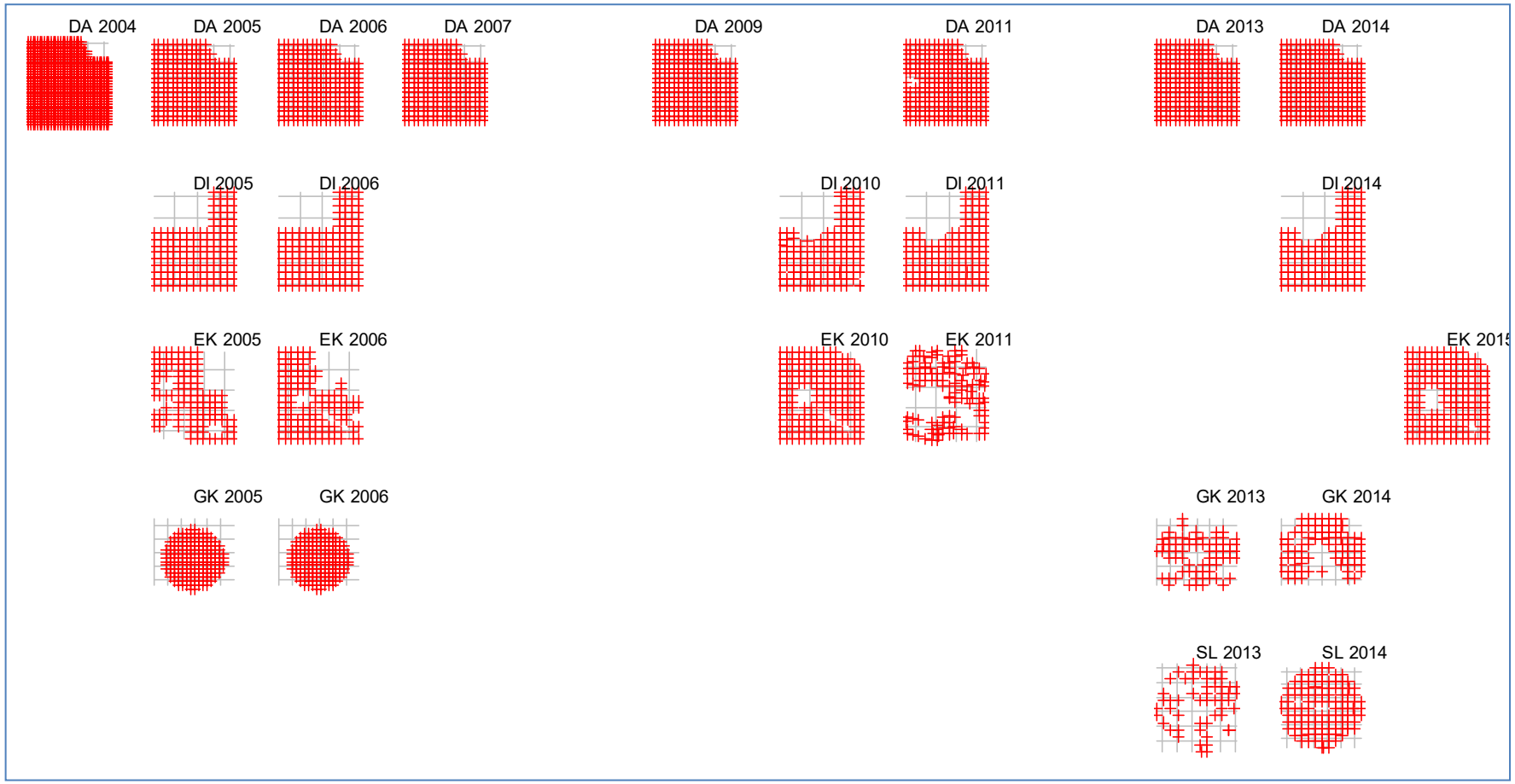

Figure 2. Temporal variation in distribution of posts for DNA sampling of wolverines in NWT in years 2004–2015 (columns) for each of five sampling sites (rows) Daring Lake (DA), Diavik (DI), Ekati (EK), Gahcho Kué (GK) and Snap Lake (SL). Post locations are shown as red crosses. Grey lines show 10-km grid – scale varies between rows. Posts were 3 km apart except for Gahcho Kué and Snap Lake in 2013–2014. At Daring Lake in 2004 the 3-km post grid was shifted 1.5 km between secondary sessions, ultimately sampling all points on a 1.5-km grid. No sampling was done in 2008 or 2012.

Details of sample collection and processing followed Mulders et al. (2007). Individuals were identified from seven microsatellite markers, and sex was determined from segments of the SRY and ZFX/ZFY genes (Mulders et al. 2007). The quality assurance methods of Paetkau (2003) were used to ensure the accuracy of individual identifications.

Data provenance and preparation are described in Appendix 1.

Spatially Explicit Capture–recapture Density Estimates

SECR methods and related terminology are introduced in Appendix 2. In this section we specify features common to the SECR analyses in the main text. SECR analyses used the maximum likelihood methods in R package SECR 3.1.4 (Efford 2018a).

The spatial population model included wolverines centered within a 40-km buffer radius of any post. Each habitat mask was discretized as 3-km square pixels. These choices are explained in Appendix 5. Estimates of sampling variance (SE and confidence intervals) were computed on the assumption that the number of wolverines in the area of each habitat mask (N) was fixed and the number of individuals detected n was binomial with size $N = D$-hat x A, where A was the area of the mask. This yields narrower confidence intervals than the default 'SECR' method in which both N and n are Poisson variables[1].

We used a detection function that treated the cumulative hazard of detection as a three-parameter 'hazard-rate' function of the distance between an activity center and a post[2]. This slightly arcane choice of detection model is justified in Appendix 4, where other possibilities are considered. The three parameters are λ_0, σ and z; λ_0 is the intercept (notionally, the hazard of detection for a post at the activity center), σ is a spatial scale parameter (units km), and z controls the shape of the curve.

Variations on the null model (the model with constant λ_0, σ and z) generally had little or no effect on estimates of overall density. There was evidence for a site-specific learned response (wolverines were more likely to be detected in the second session each year at sites they had visited in the first session), but this had negligible effect on density estimates and is not included in other models.

The data comprised 24-year x site datasets. In the terminology of the 'SECR' package, each comprised a single sampling session with multiple sampling occasions (two or four). The duration of sampling was short (<1 month) so we could consider the population demographically closed within each session. 'Session' here relates to a primary session in the robust design, and 'occasion' to a secondary session in the robust design (Pollock 1982).

We first performed a separate SECR analysis for each single-session dataset. Density and detection parameters were treated therein as specific to each site and year.

---

[1] A downside of the binomial method is that the estimated variance depends on A which is controlled by the buffer width. For very large buffer widths the two variances (binomial and Poisson) are the same.

[2] The function is $\lambda(d) = \lambda_0\ (1-\exp((-d/\sigma)^{-z})$ where d is the distance between post and activity centre. The corresponding probability is $g(d) = 1 - \exp(-\lambda(d))$. There is no connection between this use of λ and later use of that symbol for the rate of population increase.

We next conducted a pooled analysis for the northern sites (Daring Lake, DA; Diavik, DI; and Ekati, EK) assuming constant detection parameters across years while allowing for varying post layouts. Data were included for each year in which at least two of the three sites were surveyed (2005, 2006, 2010, 2011, 2014). Density was allowed to vary separately in each year but was assumed homogeneous across sites within a year. The rationale for this analysis was that the three adjoining sites sampled overlapping populations, and that pooled analysis provided a precise estimate of the regional population density in each year.

Variation in Density Among Sites

A spatially stratified SECR analysis was performed to assess evidence for site-to-site variation in wolverine density. Alternative stratifications were considered as shown in Figure 3.

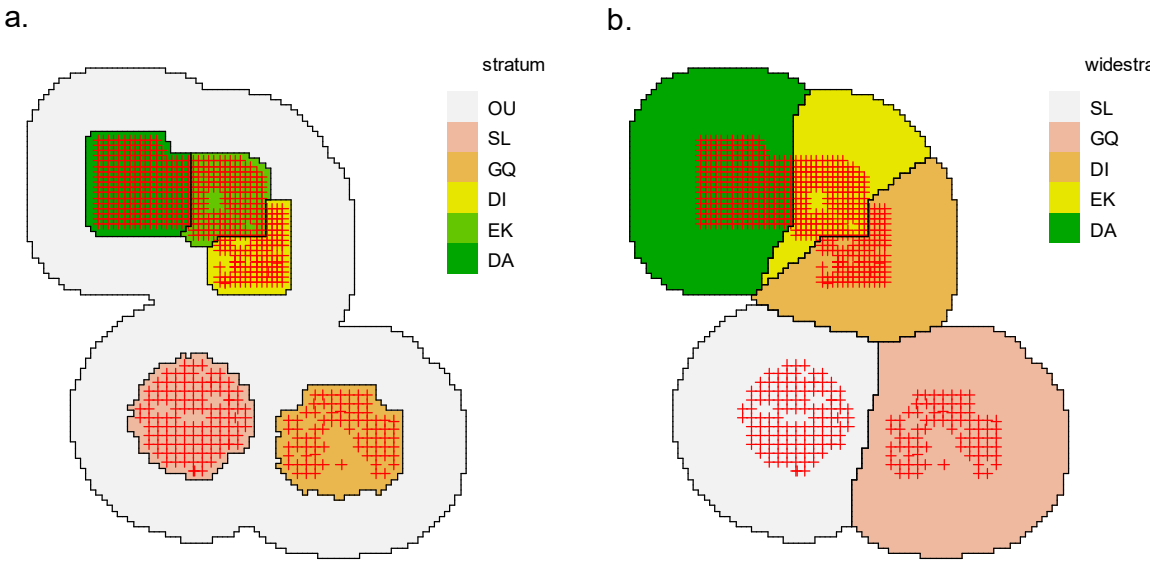

Figure 3. Alternative models for the stratification of wolverine density sampled by post grids in NWT. (a) One stratum for the immediate vicinity of each grid, plus an outer stratum (OU). (b) Partition of the overall habitat mask (40-km buffer) according to the closest post grid. Red crosses indicate post locations used in 2014–2015.

For each year in which more than one stratum was sampled we fitted a SECR model with stratum as a categorical covariate of density. That is, we estimated a separate density for each stratum. Detection parameters were assumed to be constant across strata in any one year. A likelihood ratio test was used to determine whether the fit of each stratified model was an improvement over a model with constant density across strata.

Sex Ratio

Male wolverines tend to have larger home ranges than females, and this was directly allowed for in earlier SECR models for NWT wolverine data from 2005–2011 (Boulanger and Mulders 2013a). For simplicity we omitted sex from the preceding density and trend analyses, as it had negligible effect on the estimates (Appendix 5). The preceding site-specific

and pooled analyses were also repeated with sex-specific detection parameters to assess sex effects and obtain an unbiased estimate of population sex ratio. For analyses of sex ratio, the population was treated as a mixture of two classes, with a mixing parameter for the probability a randomly chosen individual belonged to each class[3]. The mixing parameter is the sex ratio, a ratio of densities. Sex ratio was fitted as a parameter in the model; evidence for variation in sex ratio at the pooled northern sites was assessed with a likelihood ratio (LR) test comparing a null (constant-sex ratio) model to a model with year-specific sex ratio model.

Trend in Density

The preceding analyses focused on estimating wolverine population density in particular years. For monitoring we also wish to measure trend in density across years. We measure trend as the multiplier lambda (λ) by which density changes from year to year: $\lambda > 1.0$ represents an increase and $\lambda<1.0$ represents a decrease (λ is also called the finite rate of population increase). λ may be estimated annually, or as a persistent trend across multiple years.

Trend estimates may be derived from a chain of closed-population SECR estimates of density (i.e., the longitudinal analyses in (2) above). The fact that some of the same individuals appear in successive years is ignored. Multi-session SECR models may be parameterized to estimate both annual λ and a constant- λ multi-year trend (Efford 2017c).

A more comprehensive approach that allows for the *in situ* survival of some animals is to model turnover (mortality and recruitment) along the chain of samples in an "open population" model. Both apparent survival of individuals (φ) and population trend (λ) may be estimated directly from various non-spatial open population models (Schwarz and Arnason 1996, 2017). We used a robust-design implementation of the POPAN[4] model in package openCR 1.1.1 (Efford 2018b). Spatial (SECR) extensions of the open-population model are also available in openCR, but these are slow to fit and were not needed. Trend results are compared for non-spatial open-population models and spatial multi-session closed-population models. λ was expressed as an annual rate, allowing for the varying number of years between samples.

Power Analysis for Ongoing Studies

We evaluated options for annual and less frequent sampling by simulating a study with the current grid with 3-km post spacing across the present Daring Lake, Diavik and Ekati sites, and an alternate grid with 5-km post spacing over an area extended by 12 km in all directions (Figure 4). The alternative grid was 1.9 times larger in area than the current grid despite the reduction of the number of posts sampled from 584 to 406. We conducted simulations to predict the power of sampling designs to detect trend using the two levels of detector

[3] Confidence limits were back transformed from symmetrical (Wald) limits on the link (logit) scale, using the asymptotic variance estimates, as for other parameters (Efford 2018a).
[4] openCR uses the label 'JSSA' (Jolly–Seber–Schwarz–Arnason) for the POPAN model, following Pledger et al. (2010)

spacing, two levels of initial density (1.5/1,000 km^2, 3/1,000 km^2 within a 40-km buffer), and five levels of sampling frequency (one, two, three, four, six years between surveys). Power was expressed as the probability of detecting a decline in density over a 12-year period when the true rate of decline was 5% per annum ($\lambda = 0.95$) given a test with $\alpha = 0.2$ (Boulanger and Mulders 2013b). Process variance (random annual variation in population density) was not modelled.

Data were generated under a spatial model – for each replicate an initial random-uniform spatial population was generated and subjected to turnover ($\sigma = 0.67$, $\lambda = 0.95$) for 12 years (secr function sim.popn) and spatial sampling was simulated in the initial year and subsequently at the desired frequency, resulting in 13, seven, five, four or three surveys over the period. Each spatial sample was simulated with SECR function 'sim.capthist' using the hazard-rate SECR detection model with lambda 0 = 0.33, sigma = 8.6 km, z = 4.8 (obtained by averaging site- and year-specific estimates) for two secondary sessions in each sampling year (primary session). A non-spatial open-population trend model was fitted to estimate φ and λ from each spatial dataset. Decline was inferred when the upper $\alpha = 0.2$ confidence limit of λ was less than 1.0.

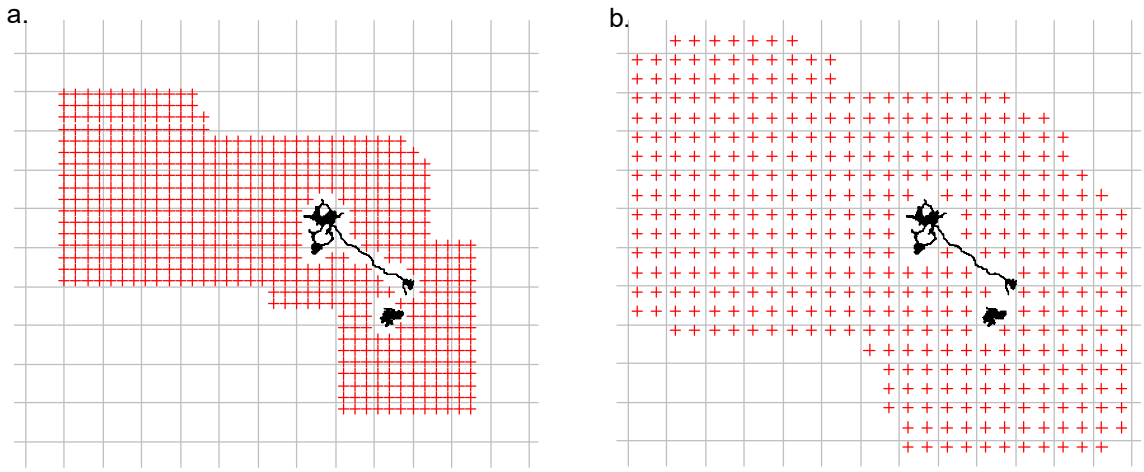

Figure 4. Grids used for simulations of varying sampling intervals: (a) 584 posts spaced 3 km apart, and (b) 406 posts spaced 5 km apart. The area is that of the current DA, EK and DI grids, excluding points within 2 km of the nominal mine footprints as shown.

Software

Analyses were performed in R 3.4.3 (R Core Team 2017) using packages **SECR** 3.1.4 (Efford 2018a) and **openCR** 1.1.1 (Efford 2018b). Annotated R code for the analyses is available from the authors as an Rmarkdown file.

RESULTS

General

The combined sample comprised 4,877 detections of 256 wolverines (116 females and 140 males). These were distributed reasonably evenly over grids and years, after an initial blip at least partly due to the more intensive sampling at Daring Lake in 2004 (Table 2).

The DA and EK grids had a common boundary, as did the EK and DI grids, and some home ranges overlapped more than one grid. Wolverines recorded on more than one grid in a given year caused the combined total in Table 2 to be less than the sum of the grid-specific counts. Some wolverines also moved between widely separated grids. Appendix 5 plots the 27 instances where the detection locations of an individual in any one year spanned more than 40 km. The most extreme example was male K14a24231 that was detected successively on the DI, DA and SL grids over little more than one month in 2014; the total distance travelled was at least 276.9 km (Appendix 5, Figure 5.2).

Table 2. Number of individual wolverines distinguished from microsatellite DNA at the five NWT sites in 2004–2015.

Site		2004	2005	2006	2007	2008	2009	2010	2011	2012	2013	2014	2015	All
Daring Lake	DA	53	38	33	34	.	27	.	22	.	24	22	.	119
Diavik	DI	.	24	22	.	.	.	19	18	.	.	17	.	59
Ekati	EK	.	21	18	.	.	.	24	25	.	.	.	19	69
Gahcho Kué	GK	.	17	17	.	.	.	.	.	.	18	15	.	47
Snap Lake	SL	.	.	.	.	.	.	.	.	.	13	15	.	23
Combined		53	86	76	34	.	27	40	51	.	52	62	19	256

Density Estimates for Each Site and Year

Density estimates from stand-alone analyses of wolverines are given in Table 3.

Table 3. Parameter estimates for each site x year from hazard-rate spatial detection model (stand-alone analysis of each area). *n* number of individuals; est maximum likelihood estimate; lcl, ucl 95% confidence limits. λ_0, σ and *z* are parameters of the detection function.

Site	Year		Wolverine density per 1000 km^2			Detection parameters λ_0			σ km			*z*		
Site	Year	*n*	est	lcl	ucl	est	lcl	ucl	est	lcl	ucl	est	lcl	ucl
DA	2004	53	6.69	5.43	8.26	0.32	0.27	0.38	6.17	5.54	6.87	3.5	3.23	3.8
DA	2005	38	5.08	3.9	6.62	0.37	0.28	0.50	6.59	5.47	7.94	3.42	3	3.89
DA	2006	33	6.1	4.57	8.13	0.38	0.31	0.47	7.58	6.7	8.57	4.87	4.21	5.64
DA	2007	34	5.89	4.47	7.76	0.40	0.35	0.47	9.26	8.61	9.95	5.74	5.04	6.53
DA	2009	27	4.85	3.58	6.58	0.23	0.19	0.26	13.39	12.28	14.59	13.01	9.14	18.52
DA	2011	22	2.95	2.14	4.07	0.31	0.25	0.37	11.79	10.28	13.53	5.32	4.36	6.48
DA	2013	24	3.03	2.25	4.09	0.33	0.28	0.39	12.07	10.9	13.36	5.26	4.52	6.12
DA	2014	22	2.99	2.14	4.19	0.33	0.26	0.41	10.32	9.21	11.56	4.79	4.06	5.65
DI	2005	24	5.71	3.93	8.29	0.47	0.31	0.71	7.5	6.12	9.2	4.36	3.61	5.27
DI	2006	22	7.02	4.78	10.3	0.39	0.28	0.53	7.01	5.84	8.41	5.05	4.13	6.18
DI	2010	19	6.02	3.93	9.2	0.21	0.13	0.35	7.64	5.36	10.88	4.66	3.31	6.55
DI	2011	18	4.27	2.8	6.5	0.52	0.38	0.73	6.95	5.54	8.71	4.14	3.36	5.1
DI	2014	17	2.54	1.68	3.85	0.39	0.26	0.58	12.41	9.15	16.84	4.72	3.44	6.48
EK	2005	21	6.51	4.32	9.79	0.32	0.22	0.48	6.05	4.59	7.98	3.97	3.17	4.96
EK	2006	18	4.87	3.13	7.57	0.29	0.19	0.43	8.22	6.41	10.55	4.58	3.37	6.22
EK	2010	24	4.54	3.07	6.72	0.11	0.07	0.16	13.54	8.59	21.36	5.55	3.41	9.04
EK	2011	25	6.54	4.35	9.84	0.37	0.21	0.65	6.04	4.63	7.88	3.87	3	4.99
EK	2015	19	3.88	2.6	5.79	0.30	0.22	0.42	7.79	6.42	9.45	4.16	3.42	5.06
GK	2005	17	4.41	2.88	6.76	0.26	0.19	0.35	8.06	6.79	9.55	4.71	3.77	5.88
GK	2006	17	4.56	2.93	7.08	0.22	0.15	0.33	7.75	6.13	9.79	4.49	3.42	5.9
GK	2013	18	3.65	2.4	5.57	0.34	0.21	0.57	10.24	7.68	13.64	5.25	3.37	8.17
GK	2014	15	3.12	1.91	5.09	0.15	0.08	0.29	10.79	6.94	16.75	4.75	2.61	8.63
SL	2013	13	1.95	1.17	3.24	0.35	0.19	0.62	11.78	8.41	16.49	4.2	2.81	6.27
SL	2014	15	2.14	1.18	3.91	0.78	0.01	42.79	2.37	0.16	34.2	2.12	1.33	3.39

The relative precision of stand-alone estimates (Table 4) was low for most grids with relative standard errors (sometimes called coefficient of variation) being greater than 20% for many of the yearly estimates.

Table 4. Relative precision (RSE %) of density estimates at the five NWT sites in 2004–2015 from stand-alone analyses.

(a) Site- and year-specific estimates from results in Table 3.

Year												
Site		2004	2005	2006	2007	2008	2009	2010	2011	2012	2013	2014	2015
Daring Lake	DA	10.7	13.6	14.8	14.1	.	15.7	.	16.5	.	15.4	17.3	.
Diavik	DI	.	19.3	19.8	.	.	.	21.9	21.7	.	.	21.4	.
Ekati	EK	.	21.1	22.8	.	.	.	20.2	21.0	.	.	.	20.7
Gahcho Kué	GK	.	22.1	22.7	.	.	.	.	.	.	21.8	25.4	.
Snap Lake	SL	.	.	.	.	.	.	.	.	.	26.5	31.4	.

(b) Expected precision (RSE %) if all detection parameters were known with certainty. This is the component of uncertainty due to sample size *n*.

		Year											
Site		2004	2005	2006	2007	2008	2009	2010	2011	2012	2013	2014	2015
Daring Lake	DA	9.6	11.5	13.9	13.5	.	15.3	.	15.2	.	14.1	15.3	.
Diavik	DI	.	16.5	18.4	.	.	.	19.7	19.0	.	.	16.3	.
Ekati	EK	.	18.7	19.8	.	.	.	15.7	16.8	.	.	.	18.1
Gahcho Kué	GK	.	20.0	20.2	.	.	.	.	.	.	19.2	21.3	.
Snap Lake	SL	.	.	.	.	.	.	.	.	.	20.4	19.0	.

Low precision in grid-specific estimates was primarily due to the low number of individuals detected on the grids rather than uncertainty in detection parameters (given the high detection probabilities of wolverines). In more detail, sampling variance may be approximated as a sum of two components – uncertainty inherent in binomial sampling of *n* individuals from those in the region of the habitat mask, and uncertainty regarding the detection parameters. The first component remains even when detection parameters are known with certainty, reducing the second component to zero[5]. Table 4b shows that this thought experiment leaves large uncertainty in all site-specific density estimates. For the wolverine data imprecision is mainly a consequence of the small sample sizes *n*. Uncertainty in detection parameters played a larger role for Gahcho Kué and Snap Lake in 2013 and 2014 when 5-km post spacing yielded sparser recapture data.

[5] See Borchers and Efford 2007 for formulae.

Pooled Northern Sites (DA, DI, EK)

An analysis of the density across all three northern sites yielded more precise estimates than stand-alone models. This was due mainly to the greater number of individuals in the pooled sample, but also to pooling of data for the estimation of detection parameters.

Table 5 provides the estimates from Figure 5 along with the detection parameters used for estimation.

Table 5. Wolverine density estimated using pooled data from Daring Lake, Diavik and Ekati sites in years when at least two of the three sites were surveyed. Detection parameters were pooled across years (estimates shown for 2005 apply to all years). *n* is the number of individuals detected.

Year		Wolverine density per 1000 km^2			Detection parameters λ_0			σ km			*z*		
	n	est	lcl	ucl	est	lcl	ucl	est	lcl	ucl	est	lcl	ucl
2005	69	5.57	4.71	6.59	0.329	0.301	0.36	8.17	7.73	8.63	4.08	3.88	4.28
2006	59	4.84	4.04	5.81	–	–	–	–	–	–	–	–	–
2010	40	5.06	4.02	6.36	–	–	–	–	–	–	–	–	–
2011	51	4.06	3.35	4.93	–	–	–	–	–	–	–	–	–
2014	37	3.32	2.62	4.2	–	–	–	–	–	–	–	–	–

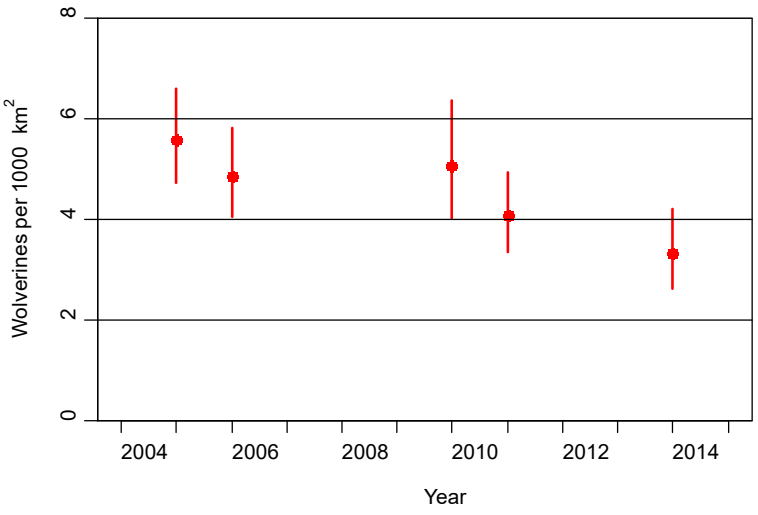

Figure 5. Wolverine density estimates for pooled northern sites in years when at least two sites were surveyed. 95% confidence intervals.

Density estimates for the entire northern region from the pooled data assuming constant detection parameters (Table 5) were substantially more precise than those from site-and year-specific models (Tables 3, 4): relative standard error (not shown) was in the range 0.09–0.12.

The estimates of detection parameters from the fitted SECR models can be used to predict the probability that a wolverine centered at a particular point will be recorded at least once. Contouring of these values provides an overall picture of how the spatially distributed

wolverine population is sampled by the post grids. We constructed such a plot using a notional combined northern grid (Figure 6).

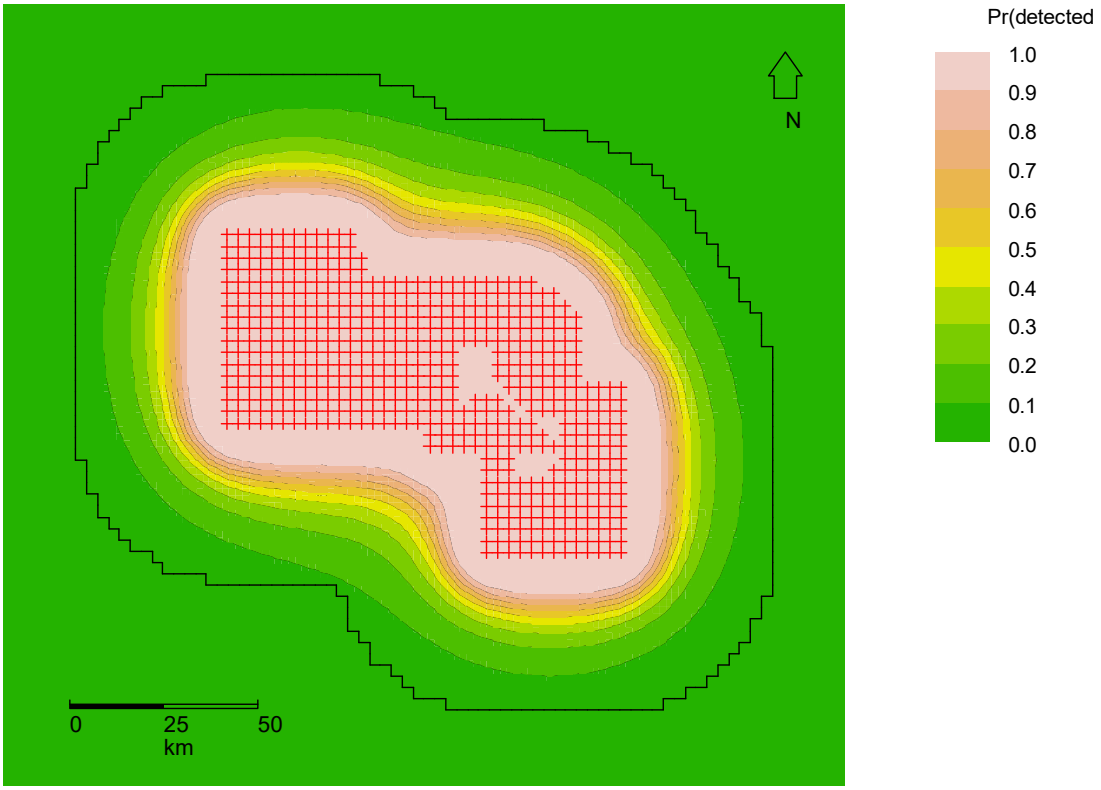

Figure 6. Contours of probability that a wolverine will be detected at least once in a survey with two secondary sessions. Red crosses indicate a grid using the post locations from DA and DI in 2014 and EK in 2015. SECR detection parameters followed Table 5. Black line shows the boundary of a habitat mask with a 40-km buffer around the detectors, as used in all analyses. Under the model all animals centered within 10 km of a post have >90% chance of being detected, but posts also detect many animals from the surrounding area, with lower per capita probability.

Variation in Density Among Sites

We did not find evidence for significant density differences among sites. All likelihood ratio tests for homogeneous vs site-specific density within years returned $P>0.2$ (Table 6). The likelihood ratio test compares the relative fit of site-specific density models with a model that assumes constant density for all sites. A non-significant result suggests minimal support for the model with site-specific densities.

Table 6. Likelihood ratio tests comparing stratified and unstratified models of density for each year in which multiple sites were sampled.

Narrow strata		Wide strata					
Year	Strata	X^2	df*	P	X^2	df	P
2005	DA, DI, EK, GK	4.22	4	0.38	3.45	3	0.38
2006	DA, DI, EK, GK	2.65	4	0.62	1.69	3	0.64
2010	DI, EK	2.97	2	0.23	0.00	1	0.95
2011	DA, DI, EK	1.94	3	0.58	1.04	2	0.60
2013	DA, GK, SL	1.39	3	0.71	1.63	2	0.44
2014	DA, DI, GK, SL	5.33	4	0.25	1.86	3	0.60

* Narrow strata include an additional 'outer' stratum in all cases, hence extra df.

Stratum-specific estimates for each multi-stratum year are shown in Figure 7.

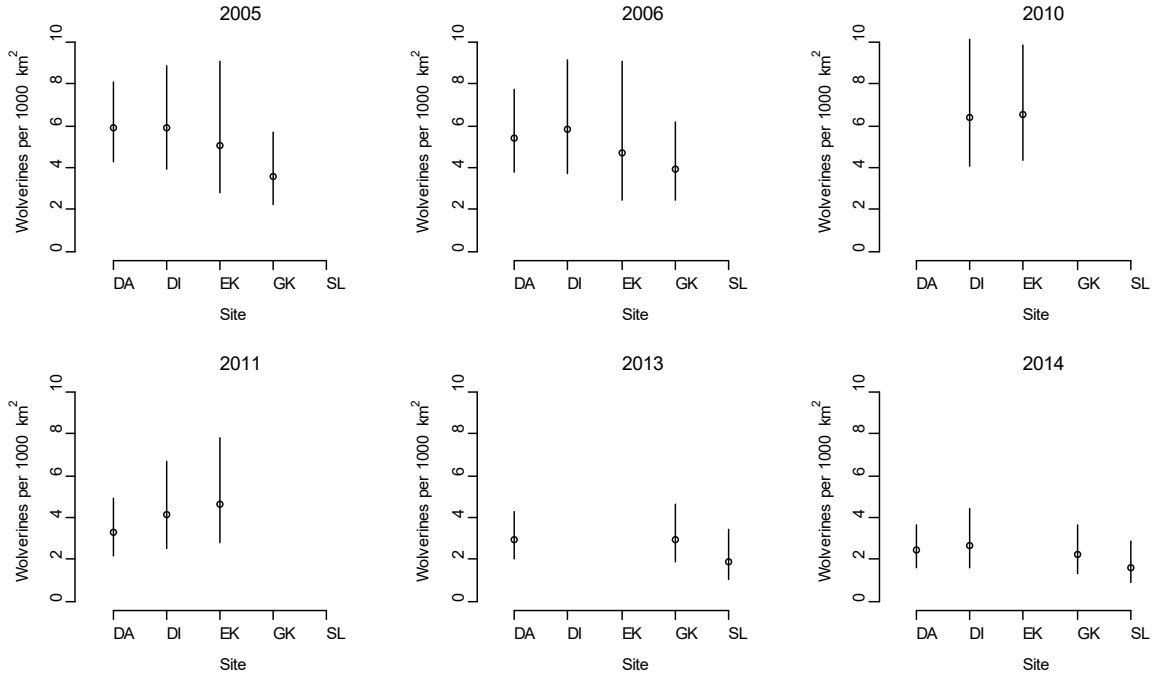

Figure 7. Stratum-specific wolverine densities (wide strata including outer zone) in years when more than one stratum was sampled. 95% confidence intervals. Detection parameters were shared across strata. The 'wide' definition of strata is shown because these estimates were more precise.

Although a pooled estimate of wolverine density in 2014 in the northern strata (DA + EK + DI: 2.53 per 1,000 km^2, 95% CI 1.90–3.36 per 1,000 km^2) was slightly more than in the southern strata (SL + GK: 1.90 per 1,000 km^2, 95% CI 1.3–2.70 per 1,000 km^2) the difference was far from significant (LR test X^2 = 1.16, df = 1, P = 0.28).

Sex Ratio

Although more males were detected than females over the study as a whole, the estimated sex ratio was even or female-biased in most sites and years (Figure 8). Sex-specific detection

models allowed for the longer movements of males. The effect in most cases was to increase the estimated proportion of females in the population (Appendix 4). Confidence intervals were wide because few individuals were present at each site. Female bias was most marked at Diavik and apparently absent at Daring Lake.

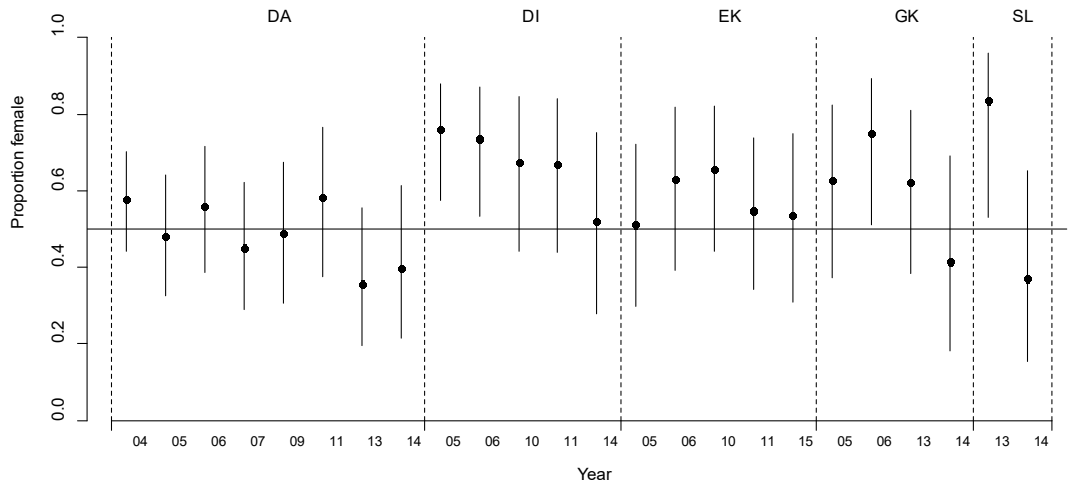

Figure 8. Wolverine sex ratio estimates from sex-specific detection model fitted separately for each year at five sites in NWT. 95% confidence intervals.

Overall population sex ratio at the pooled northern sites (DA, DI and EK) was 56.3% female (95% CI 50.1–62.3%). There was no evidence for variation among years in the sex ratio at these sites (LR test X^2 = 1.0, df = 4, P = 0.8). We did not formally assess sex-ratio variation among sites.

Trend Models

Population trend estimated with open-population non-spatial models agreed closely with the trend in densities estimated by SECR (Table 7). There was clear evidence that density declined over 2004–2014 at DA, and slightly weaker evidence for decline over 2005–2014 at DI (Figure 9). There was no evidence for overall decline at EK (2005–2015) or GK (2005–2014). Increases in the extent of these grids over time may have caused positive bias in the non-spatial (JSSA) λ–hat and obscured minor declines. However, very similar estimates of λ were obtained by SECR which controls for changing extent. Data from SL spanned only 2013–2014 and the one-year estimates of λ were uncertain and inconsistent.

Table 7. Overall population trend of wolverines at five sites in NWT estimated using either non-spatial Jolly-Seber-Schwarz-Arnason models (JSSA) or density model in 'secr' (SECR). 95% confidence intervals in parentheses. JSSA model (φ∼session, λ∼1, p∼session)

Site	Period	λ–hat (JSSA)	λ–hat (SECR)
Daring Lake	2004–2014	0.910 (0.868–0.954)	0.932 (0.898–0.967)
Diavik	2005–2014	0.965 (0.901–1.035)	0.964 (0.908–1.024)
Ekati	2005–2015	1.001 (0.945–1.061)*	0.982 (0.931–1.035)
Gahcho Kué	2005–2014	1.010 (0.940–1.086)†	0.990 (0.933–1.051)
Snap Lake	2013–2014	1.154 (0.636–2.093)	0.876 (0.416–1.845)

* JSSA lambda for Ekati includes artefact from increase in sampling area between 2006 and 2010.

† JSSA lambda for Gahcho Kué includes artefact from increase in sampling area between 2006 and 2013.

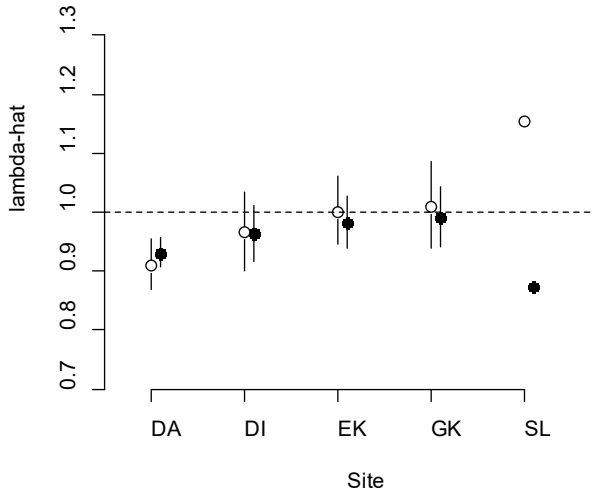

Figure 9. Overall site-specific trend in density estimated by two capture–recapture methods (non-spatial open circles; spatial-closed circles). Results from Table 7. 95% confidence intervals (not shown for SL as spanned y-axis for both methods). Model (φ∼session, λ∼1, p∼session).

Inspection of apparent survival (ϕ) and per-capita recruitment (f) suggested similar apparent survival across areas but higher per-capita recruitment for Diavik and Ekati compared to Daring Lake (Figure 10). Per-capita recruitment, in the context of open models, could be due to either births of wolverines or immigration of wolverines into the study areas. Estimates of per-capita recruitment and λ for EK and GK should be interpreted cautiously due to change in the study area layout over the course of the survey (Figure 2).

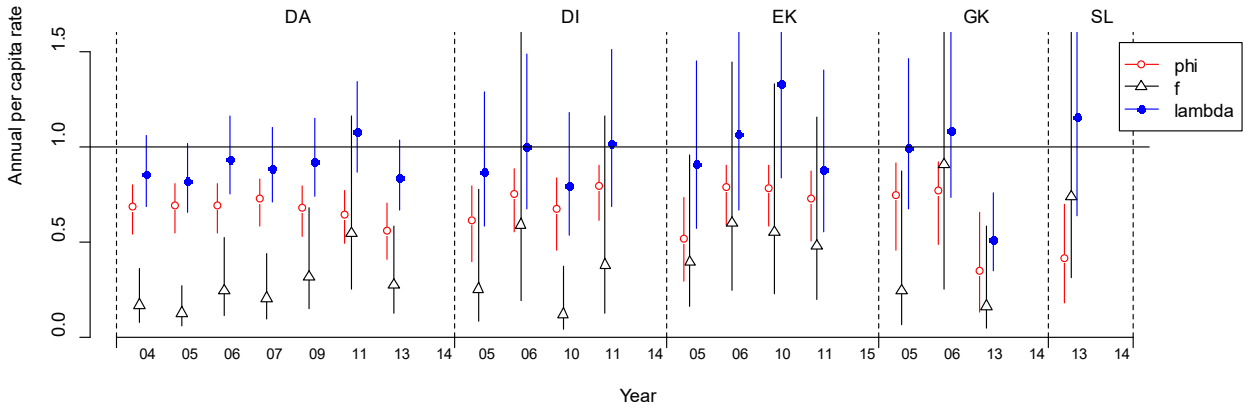

Figure 10. Components of annual change in wolverine populations sampled across multiple years (apparent survival, phi; per capita recruitment, f; finite population growth rate, lambda). Sexes pooled. Estimates relate to the one to seven year period following the year on the x-axis. 95% confidence intervals.

Estimates of apparent survival (φ) were greater for females than for males in all areas, discounting the weak estimate from SL Lake (Table 8). About 25% of females and 35% of males disappeared (due to emigration or mortality) in each year.

Table 8. Apparent survival from non-spatial Jolly–Seber–Schwarz–Arnason model (φ~sex, λ~1, p~session+sex). 95% confidence intervals in parentheses. All values expressed as annual rate

			Apparent survival	
Site	Period	Years	Females	Males
Daring Lake	2004–2014	10	0.732 (0.657–0.795)	0.673 (0.591–0.745)
Diavik	2005–2014	9	0.781 (0.683–0.855)	0.655 (0.535–0.758)
Ekati	2005–2015	10	0.732 (0.625–0.818)	0.692 (0.578–0.787)
Gahcho Kué	2005–2014	9	0.767 (0.545–0.900)	0.597 (0.351–0.803)
Snap Lake	2013–2014	1	0.377 (0.135–0.702)	0.464 (0.183–0.771)

Study Design

Post Spacing at Gahcho Kué

Post spacing at GK was increased from 3 km in 2005–2006 to 5 km in 2013–2014, while post number was reduced from 175 to 68 (2013) or 79 (2014) (Figure 11). Wider spacing increased the area sampled and hence the number of individuals detected remained about the same, despite lowered sampling intensity. Despite the reduced number of recaptures, which increased the imprecision of detection parameter estimates (cf Table 4b), the precision of density estimates was little changed (Table 9).

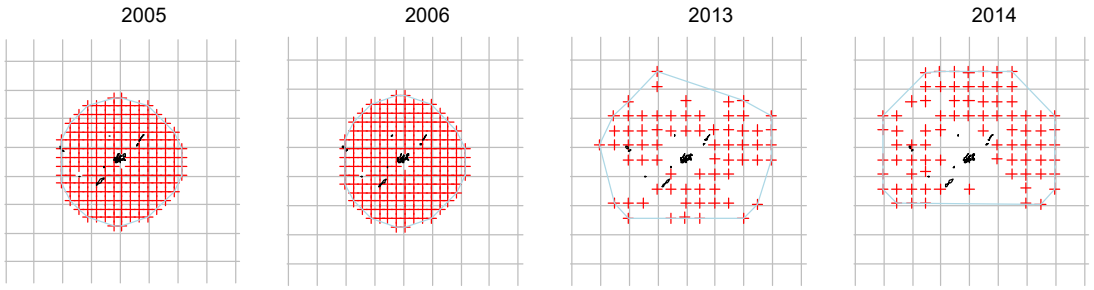

Figure 11. Distribution of posts at GK. 10-km grid lines. Nominal mine footprint shown in black.

Table 9. Comparison of wolverine density estimates at Gahcho Kué with two post spacings. *n* = number of individuals detected; *r* = number of re-detections, RSE = relative standard error of estimate (aka CV). 'Area' is the area of a convex polygon bounded by the outermost posts.

	Spacing km	Number	Area km²	n	r	D-hat per 1000 km²	RSE(D-hat) %
2005	3	175	1467	17	135	4.41	22.1
2006	3	175	1467	17	88	4.56	22.7
2013	5	68	2353	18	47	3.65	21.8
2014	5	79	2455	15	33	3.17	25.4

Simulations of Varying Post Spacing and Sampling Interval

Simulation results are summarized in Figure 12. The estimated λ from the constant-λ non-spatial JSSA model showed a small, consistent negative bias. Estimated φ showed a larger bias, especially when sampling was intensive. We attribute these effects to the individual heterogeneity in detection probability *p* introduced by spatial sampling, but further simulation is needed. The precision of the λ estimates was almost unaffected as sampling interval increased from one to six years, but was impacted by reduced sample size in the lower-density scenario.

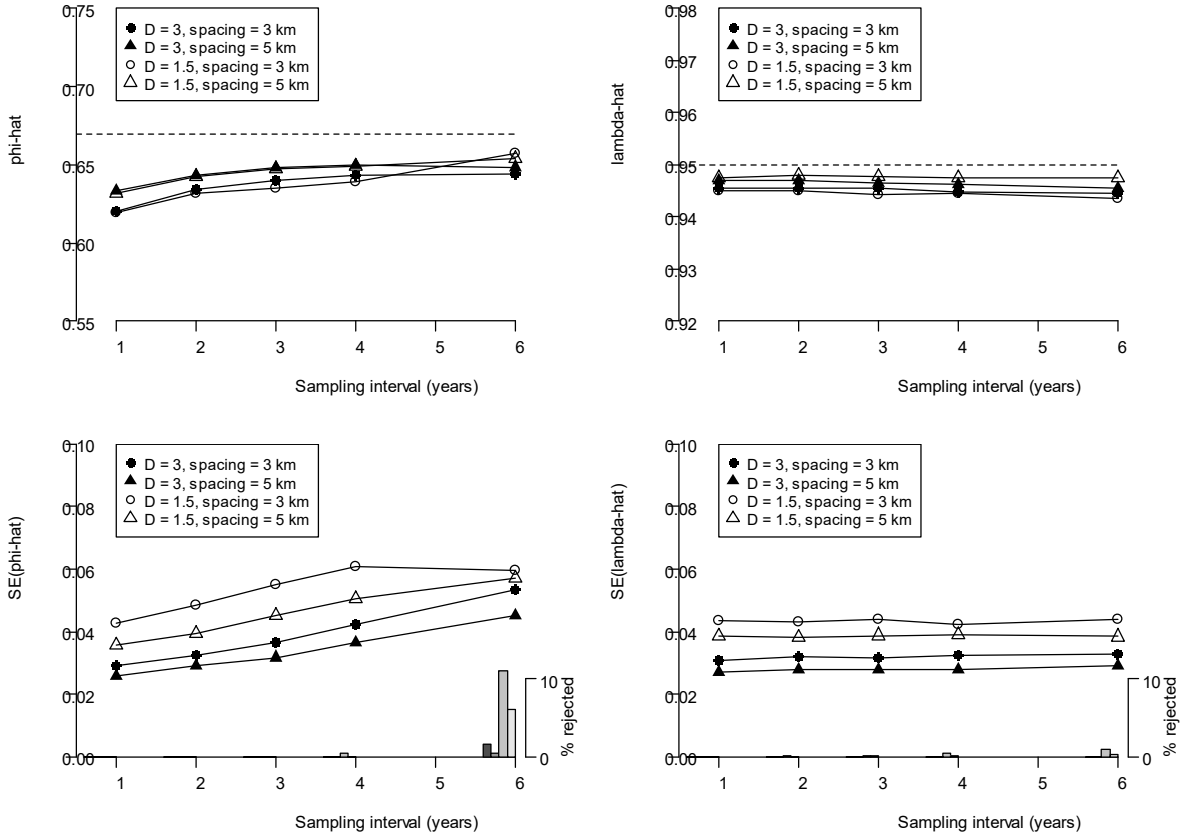

Figure 12. Mean and SD of estimates of apparent survival (phi) and population growth rate (lambda) from simulated sampling for two initial densities, two post spacings (3 km, 5 km extended grid) and five sampling intervals. Dashed lines indicate true phi and lambda. At large sampling intervals a fraction of simulations fail because of a lack of recaptures; these estimates (φ<0.2 or λ<0.2) were rejected from the summary statistics as shown (bars in the same order as scenarios in legend; reject applied for both mean and SE).

The power to detect 5% annual decline was strongly dependent on density (Figure 13). The slightly greater precision of φ and λ estimates with 3-km spacing translates to greater power to detect the downward trend – about 6% more power under each scenario for sampling interval and density (Figure 13).

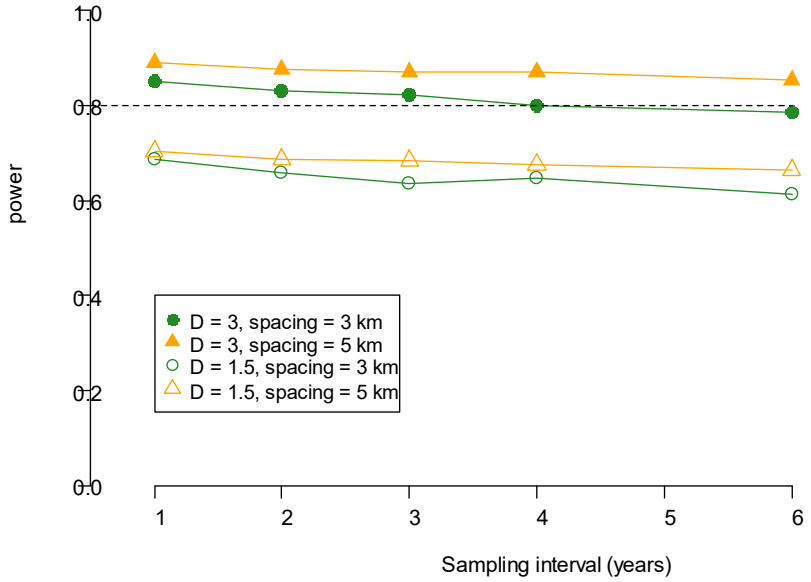

Figure 13. Power to detect 5% annual decline in wolverine density under the sampling scenarios in Figure 12. $\alpha = 0.2$.

DISCUSSION

Differences from Previous Analyses

Previous analyses included estimates of superpopulation size. We rely entirely on density estimates because the conventional concept of population size is problematic for spatially distributed populations when there is no natural boundary to define the population. The size of the 'superpopulation' increases the more sampling is done, so it is not a useful concept. The number of wolverines centered in a specified geographic region may be predicted from the density model (Efford and Fewster 2013), but we did not attempt this as natural regions were not specified[6].

Spatial Variation in Wolverine Density

We found it difficult to measure density separately at the control site (DA) and nearby mine sites (DI and EK). This is a combined effect of the large scale of wolverine movements, the sparseness of the population, and the proximity of the sites, as illustrated in Figure 14. Most wolverines detected on each grid currently have centres off the grid. For example, the expected numbers of wolverines centered on each grid in 2014–2015 were 7.6, 3.1 and 6.4 (using the nominal area = number of posts x spacing^2, and density estimates from Table 3), or only 18–35% of the numbers observed (22, 17, 19; Table 3). Several wolverines are vulnerable to detection on two grids and cannot be assigned to one or the other from their detection locations.

[6] We use the approach later to infer the expected number of centres on each nominal northern grid.

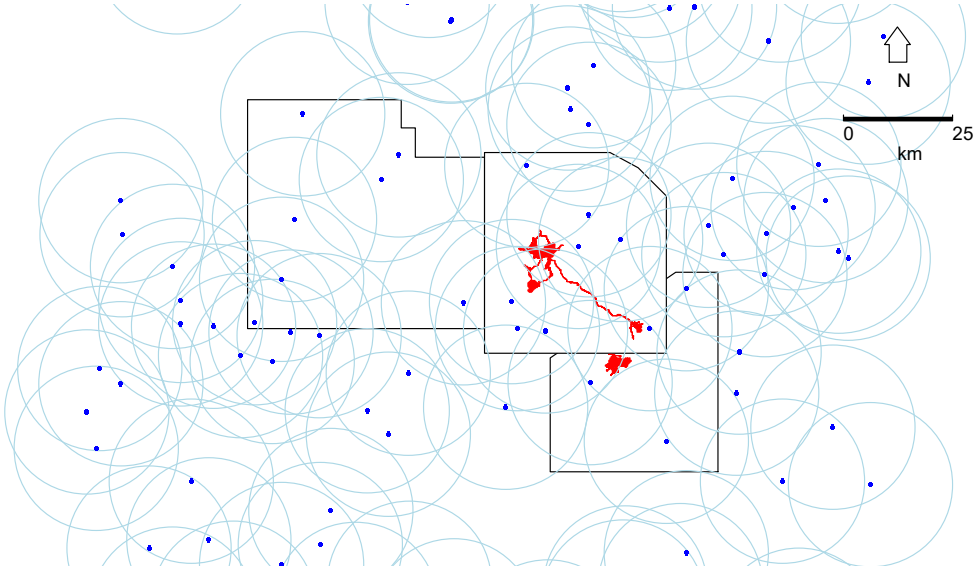

Figure 14. Simulated random distribution of wolverine activity centres (blue dots; 3 wolverines per 1,000 km^2) with notional 19-km radius home ranges (light blue circles). Footprints of EK and DI mines shown in red. 19 km is the radius that includes 95% of activity under the average hazard-rate detection function (σ = 8.6 km, z = 4.8; Table 3 and function circular.r in package 'secr').

Sex Ratio

Wolverine sex ratio was generally female-biased. Female-biased sex ratio is expected in mammals because of the near-even sex ratio at birth and earlier senescence of males. The greater number of males distinguished from DNA is a combined result of the larger home ranges of males, which results in males being sampled from a larger region than females, and possibly also a greater propensity for natal dispersal and transience. There was weak evidence that the sex ratio was persistently less female-biased at Daring Lake than at other sites, or completely unbiased. This may be a clue to spatial variation in age structure, source-sink dynamics or other inhomogeneity.

Trend in Wolverine Density

There appears to have been a decline in density over 2004–2014, especially between 2009 and 2011 on the Daring Lake grid. Sampling on that grid followed a very consistent design except for the reduction in duration and intensity between 2004 and 2005. If transient wolverines were a significant fraction of the population, then the longer duration of sampling in 2004 may have inflated the estimates. However, wolverine density at Daring Lake continued to decline after 2005.

We do not have the necessary background information to interpret the decline. An effect of caribou population dynamics seems likely, but human harvest may also be involved. Harvest levels were higher for Daring from 2005–2009 with five females and five males being removed during 2005–2009 compared to five males for Ekati and Diavik (Boulanger and Mulders 2013a). We note a theoretical possibility that the baited-post survey methodology itself may have induced a change in late winter wolverine distribution or survival.

Other grids analyzed alone provided weak evidence of decline (DI) or no evidence (EK, GK). Care is needed in attaching significance to this negative result because the sampled northern populations overlap substantially, and the datasets differ in their power to detect change (much more work was done at DA). The difficulty of distinguishing local trends in density among sites is inherent in the species' biology (low density, large movements) and the logistical constraints on the location of a control area for comparison. In retrospect, one might have wished for a more distant control site or sites than DA. Our advice at present is to continue monitoring change over time in the combined population while investigating the dynamics in more detail at the level of individual behaviour.

Study Design

The design pioneered at DA has proved highly effective for sampling wolverine populations, and Mulders et al. (2007) rightly stressed the need for consistency in design from year to year. However, the cost of each annual survey is considerable, and it is reasonable to ask whether a similar or better outcome could be achieved for less cost. We observe –

1. The basic design using two ten-day sessions yields large numbers of detections, and we see no reason to change this.
2. A consistent rule should be applied for the number of samples analysed per post where there are multiple hair samples. We do not have evidence that this much affects the population estimates, but it is desirable to maintain a constant protocol. The NWT studies have mostly selected a single sample per post, and that should be continued.
3. Distinguishing density trends at the DA, EK and DI sites is almost impossible because wolverines are so mobile: there are no natural lines dividing these populations. At low densities, such as apply at present, the stratification approach is unable to discern differences in densities between the study areas. However, the stratification approach effectively considers movements of wolverines across study boundaries therefore providing a more robust estimate of wolverine density for the larger study area.
4. We suggest that sampling years are synchronized across study areas to maximize the sample size of wolverines, thereby increasing overall precision of estimates.

The two main areas for possible economies are post spacing (and the related question of study area extent), and whether sampling should be conducted annually or at greater intervals, perhaps every two, three, or four years. We predict that an increase in post spacing to 5 km with a moderate (12 km) extension in the perimeters of the DA, EK and DI grids would result in improved precision given that the area sampled would be increased by a factor of 1.93 therefore increasing the number of wolverines sampled. The cost of visiting each post increases when they are further apart, so savings would presumably be less than implied by the 30% reduction in number of posts.

Our simulations showed that widely spaced sampling times, even up to six-yearly, can give accurate estimates of long-term trend in density. However, precision of the trend estimate is not the only relevant criterion, and there may be good reasons for more frequent monitoring:

- Frequent monitoring is needed to give a timely warning of an abrupt decline in wolverine density. Power analyses that we conducted assume a constant trend.
- If management action is taken to increase the present low densities, then short-term feedback on the success of that action is desirable.
- Estimates of per capita recruitment and apparent survival become much less precise when the sampling interval is extended. Precise estimates are needed to interpret wolverine population dynamics and choose among management options.

ACKNOWLEDGEMENTS

Funding for this research was provided by the Government of the Northwest Territories (GNWT) – Environment and Climate Change, the West Kitikmeot Slave Study, Indian and Northern Affairs Canada - Renewable Resources and Environment Directorate, BHP-Billiton Ltd., Diavik Diamond Mines Inc., and DeBeers Canada Ltd.

The collection of wolverine genetic samples involved many individuals working for BHP Billiton, Diavik Diamond Mines Inc., DeBeers Canada, and the Department of Environment and Climate Change. Specifically, BHP Billiton personnel included Brent Murphy, Elizabeth Miller, Jorgen Bolt, Patrick Kramers, David Abernethy, Maurice Boucher, Ross Lehune, Charles Klengenberg and Scotty McLeod. Diavik Diamonds Inc. personnel included Scott Wytrychowski, Scott Morrison, Colleen English, Seth Bohnet, Karl Cox, Ray Eskelson, George Taptuna, Bobby Algona and Peter Katiak. Individuals working for DeBeers Canada and/or AMEC Earth & Environmental included Robin Johnstone, Raymond Marlowe, Joseph Catholique, Derek Michel, Chris Godwin-Sheppard, Eric Hamelin, James Clark and Janet Bauman. Environment and Climate Change employees included Ray Case, Rob Gau, Dean Cluff, Dave Taylor, Paul Mackenzie, James Sangris, Patrick Charlo, Lawrence Goulet, Edward Doctor, Nap Mackenzie, Shalene deWynter, Sunny Ashcroft, Joanna Wilson, Joel Gowman, Lesley Johnson, Sarah Stevenson, Jean-Francois Dufour, Credence Wood, John Lee, Cindy Taylor, Steven Matthews and Adrian D'Hont. Many ECC staff at the North Slave regional office assisted, primarily with the collection of carcasses, including Shelly Acton, Irene LeMouel, Raymond Bourget, Janice Ziemann, Patricia Lacroix, Albert Bourque and Danny Beaulieu. Golder Associates conducted preliminary analyses of data from the Diavik study area for DeBeers Canada.

David Paetkau, Tobi Anaka, Paul Sylvestre, Catherine Littlewood, Jessica Wastl, Jennifer Weldon conducted extraction and genotyping at Wildlife Genetics International Labs in Nelson BC.

APPENDIX 1. DATA MANAGEMENT

Data for DA, DI and EK in the years 2005, 2006, 2010, and 2011 had been prepared as text files in the DENSITY input format (Efford 2012) for the earlier analyses of Boulanger and Mulders (2013a). Post locations were in the files 'DL2005.txt', 'DL2006.txt', 'DL2011.txt', 'DI2005.txt', 'DI2006.txt', 'DI2010.txt', 'DI2011.txt', 'EK2005.txt', 'EK2006.txt', 'EK2010.txt' and 'EK2011.txt'. Individual detections were in the file 'DLEKDIKL_areayearsess.txt'. Corresponding data for GK (aka Kennady Lake) in 2005 and 2006 were in the files 'KL site utms.txt' and 'Kennady0506_captsex.txt'. Further Daring Lake data from 2004, 2007 and 2009 were provided in the R binary file 'Daring2004_11.RData' (Boulanger and Mulders 2013b).

Data for 2013–2015 were input from various Excel spreadsheets as follows.

Post Locations

'Daring 2014 Wolverine DNA - April 2014_RMDec22.xlsx'
'Diavik 2014 - Wolverine - DNA - Record for ENR-Diavik 2014.xls'
'Gacho Que Snap Lake_2013-14_WV_Field_Summary .xlsx'
'Ekati 2015 Wolverine DNA Spreadsheet.xls'

Post locations were not explicitly given for DA in 2013; it was assumed they were the same as in 2014. Locations provided as unprojected latitude and longitude (WGS84; EPSG 4326) were transformed to UTM Zone 12N (EPSG 26912) using function spTransform in R package rgdal (Bivand et al. 2017). The post locations in some spreadsheets contained obvious errors (e.g. multiple posts with the same UTM coordinates); these were corrected ad hoc by inferring UTM coordinates from the row and column numbers in the post name.

Individual Detections

Data on individual detections were extracted from the spreadsheets of WGI that included detailed laboratory results.

'Daring Lake WGI g1592_2014 Results.xlsx' (includes projects g1373 2013 and g1592 2014)
'Diavik 2014 WGI g1499 Results.xlsx'
'GachoKue WGI g1512_Results.xlsx' (2013 and 2014, Gahcho Kué and Snap Lake)
'GachoKue WGI g1512_Results.xlsx' (2013 and 2014, Gahcho Kué and Snap Lake)
'Ekati 2015 WGI g1620 Results rev102317.xls'

The spreadsheets differed in the naming and ordering of columns, and in some coding details. R code was written to extract and match the necessary fields from the post-location and laboratory spreadsheets.
Data were saved as a set of 24 R capthist objects[7] named 'DA2004CH', 'SL2014CH' etc. Site codes DA, DI, EK, GK and SL are self-explanatory. The suffix 'CH' indicates a capthist object

[7] capthist objects are defined and used in the R package secr (Efford 2018a).

that includes both post locations and individual detections for the given year and site). The sex of each animal was stored as the individual covariate 'Sex' in each CH object.

Data inherited from earlier analyses (2004–2011) included a 'usage' attribute that recorded which posts were checked on each occasion (secondary session). This was particularly important for Daring Lake in 2004 when each post location was only sampled once (because posts were moved) and Ekati in 2006 when only 82 of 132 posts were checked on the second occasion. Otherwise, at least 96% of posts were checked on each occasion. Post usage for the newer 2013–2015 data was assumed to be 100% as usage data were hard to extract from the diverse spreadsheet formats and small omissions have negligible effect on estimates (M. Efford unpubl. results).

The date and duration of each sampling interval (secondary session) was not included in the final dataset as these were not available for earlier years and the diversity of formats makes them hard to extract reliably. We note that sampling intervals were often longer than the nominal duration (ten days) and durations varied somewhat (Appendix 1 Table 1.1).

Table 1.1. Duration of sampling intervals (days) 2013–2015.

	2013			2014			2015		
	Min	Max	Median	Min	Max	Median	Min	Max	Median
Daring Lake	*	*	*	1	20	10	–	–	–
Diavik	–	–	–	5	15	11	–	–	–
Ekati	–	–	–	–	–	–	10	15	12
Gahcho Kué	7	16	12	9	17	11	–	–	–
Snap Lake	10	16	13	9	23	16	–	–	–

* No data for DA 2013

If durations were available for all sites, then the variation in effort could be incorporated in analyses via the usage attribute (Efford et al. 2013).

The 24 site x year objects were combined by year or site as required for particular year-specific or site-specific analyses or bundled together as the R list 'allCH'. The binary R file 'allCH.RData' includes all the 2004–2015 capthist data at various levels of aggregation.

APPENDIX 2. AN OUTLINE OF SPATIALLY EXPLICIT CAPTURE–RECAPTURE

SECR is a statistical approach for estimating the density of a spatially distributed animal population, and for estimating trend in density over time. The data for SECR comprise spatial detection histories; each history is a record of the particular sites at which each individual was detected. Detected individuals are a filtered selection of those centered in the surrounding area – the filter is a function that relates detection probability to distance. By fitting a statistical model, we are able to estimate both parameters of the detection function and the (unfiltered) density of activity centres. SECR avoids many of the 'closure' issues that dogged previous analyses (Mulders et al. 2007).

SECR has developed over the last 15 years and now exists in two main flavours characterized as 'maximum-likelihood' (Borchers and Efford 2008, Efford 2018a) and 'Bayesian' (Royle et al. 2014).

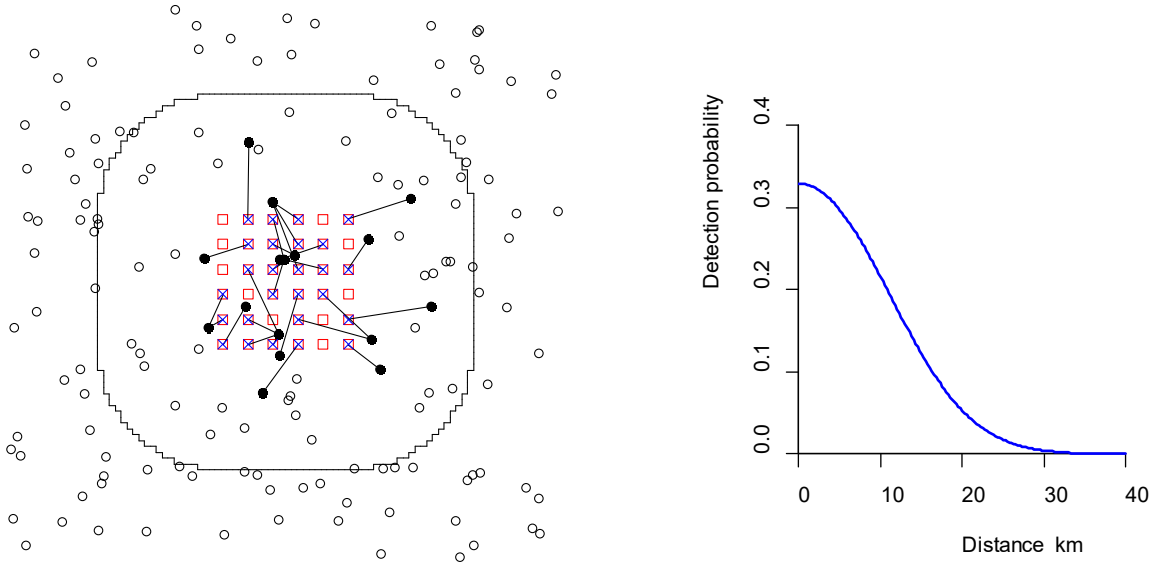

Figure 2.1. Spatially explicit capture–recapture conceptual model. Animal activity centres (dots) are distributed across the wider landscape. Animals centered near a detector (red squares) have a high probability of detection (blue crosses; see also hypothetical distance-detection function on right). The centers of animals detected at least once are shown as filled dots (a single sampling interval is shown). Animals centered beyond an arbitrary outer perimeter (solid line) have such low probability of detection that they can be ignored in model fitting.

For SECR the population is conceived as a distribution of animal activity centres in two dimensions (Figure 2.1). We can ignore centres that are very far from detectors because these animals stand negligible chance of detection, and this has computational benefits. For SECR using the method of maximum likelihood it is necessary to perform an integration over space, which is easier when space is finite and can be discretized as many small pixels. The criterion for ignoring distant animals is usually a buffer of a certain width around the detectors. The buffer is represented by the perimeter line in Figure 2.1. The area within this

boundary becomes the area of integration for maximum likelihood (or the 'state space' of centres in Bayesian models e.g. Royle et al. 2014). The term 'habitat mask' is used for the area of integration in package SECR.

Where habitat extends indefinitely in all directions, as appears to be the case for NWT wolverines, the placement of the boundary is arbitrary. The area should merely be large enough that enlarging it further has no effect on density estimates because only un-detectable animals are added. This is achieved by using a buffer around the posts that is large compared to the radius of home ranges. Whether the buffer is large enough can be tested once pilot values are available for the scale of detection σ.

APPENDIX 3. SECR MODEL FOR CAPPED DETECTORS

With rare exceptions, only one wolverine hair sample was analyzed per post from each secondary session. The data were therefore binary at the level of each post and secondary session, and animals appeared to 'compete' for posts (Appendix 2 Figure 2.1). This data type differs from all published SECR models, and specifically does not match the usual 'multi' nor 'proximity' detector types (Borchers and Efford 2008, Efford et al. 2009, Efford 2018a). We developed a probability model for the new detector type ('capped') that will be described separately (M. Efford unpubl.).

The main exceptions were at Gahcho Kué and Snap Lake in 2013 and 2014, when multiple DNA samples appear to have been analyzed from some posts.

Coding of the new detector type in SECR is incomplete, and certain models of interest for wolverines are not available in version 3.1.4 (particularly learned response models). We discovered by simulating many datasets that density estimates are largely unaffected when a 'proximity' model is used with 'capped' data. The proximity model is binary at the level of each post, animal and secondary session: it allows multiple detections at a post as long as they are from different animals.

To demonstrate the near equivalence of the 'capped' and 'proximity' estimators of density we applied both estimators to the 24-size x year wolverine datasets (Figure 3.1).

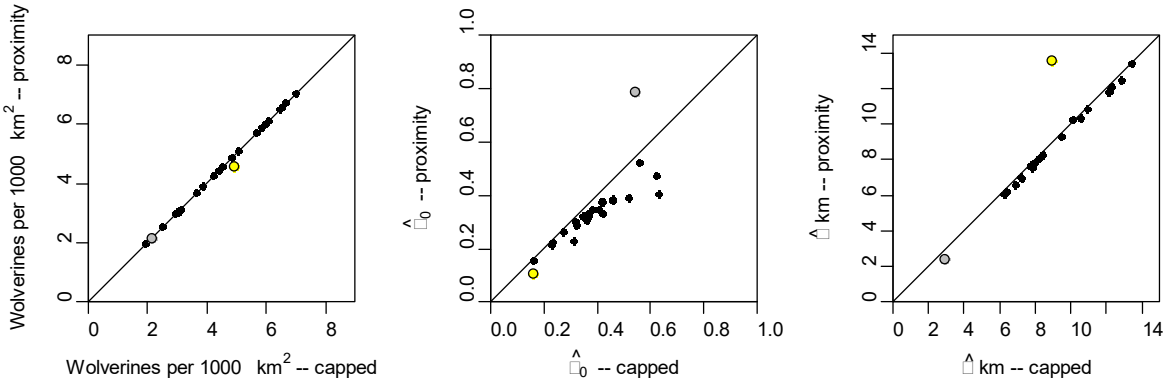

Figure 3.1. Relationship between estimates of wolverine density and SECR detection parameters using either the correct model (capped) or the simpler misspecified model (proximity). Hazard hazard-rate (HHR) detection function; parameter *z* not shown. Outlying points are for EK in 2010 (yellow)[8] and SL in 2014 (grey)[9].

[8] The discrepancy for SL2014 is probably due to the fact that more than one sample was analyzed per post, and to use the 'capped' estimator' a few detections were discarded at random to reduce the sample to one individual per post.

[9] The discrepancy for EK2010 is unexplained.

The effect of misspecification is largely absorbed by the intercept parameter of the detection function λ_0 (i.e., λ_0-hat from the misspecified model is negatively biased, while *D*-hat is nearly unbiased). In the main text we report results only from proximity-detector models.

APPENDIX 4. MODELING THE DETECTION PROCESS IN SECR

There are many ways to customize models of the detection process in capture–recapture analyses. Use of a suitable model may reduce the chance of bias in population estimates. However, the detection process has little intrinsic interest (detection parameters are mostly nuisance parameters).

Choice of model draws on both a priori understanding of biology and the sampling process, and evidence from the data themselves using criteria such as AIC. In our view, the benefits of finding a better, more complex, model show rapidly declining returns. SECR estimates are robust to many sources of variation, and reduction in bias is typically small compared to sampling error. Our approach is therefore pragmatic: find an adequate detection model that will address major known sources of bias and can be applied uniformly across multiple subsets of the data (sites, years).

Following sections address these issues:

- shape of detection function
- learned (behavioural) responses
- sex differences in detection
- difference between the two secondary sessions in each year
- variation among sites and between years (pooling of parameters)

We do not consider:

- effect of varying intervals between post checks within a year

Shape of Detection Function

A key idea in SECR is that the probability of detection declines as a detector is placed further away from the center of an animal's home range, and that the decline can be described by a simple function from a parametric family. It can be more elegant to model decline in the cumulative hazard of detection h rather than the probability of detection *per se*; probability p may be inferred from cumulative hazard using $p = 1 - \exp(-h)$. We use the hazard form.

The usual function choices are half-normal or negative exponential (each with two parameters) or the three-parameter 'hazard-rate' function [10] from distance sampling (Buckland et al. 2001). Each function has a characteristic shape; the most important differences for SECR lie in the length of the tail. For functions with a short tail such as the half-normal, the probability of detection in the periphery of the home range quickly declines to near zero.

Functions with longer tails allow occasional detections in the periphery, and hence occasional recaptures at extreme distances can be accommodated without much shifting the

[10] 'hazard-rate' here describes the shape of the function; the hazard-rate function may be used with either probability or cumulative hazard as the response.

median recapture distance. This is potentially important for the wolverine data as occasional individuals appear to be vagrant or highly mobile (Appendix 5).

We compared the fit of the three candidate detection functions for each of the 24 site x year samples. We used the form in which the cumulative hazard of detection, rather than detection probability itself, followed the parametric shape. The two forms are similar in shape, but not identical.

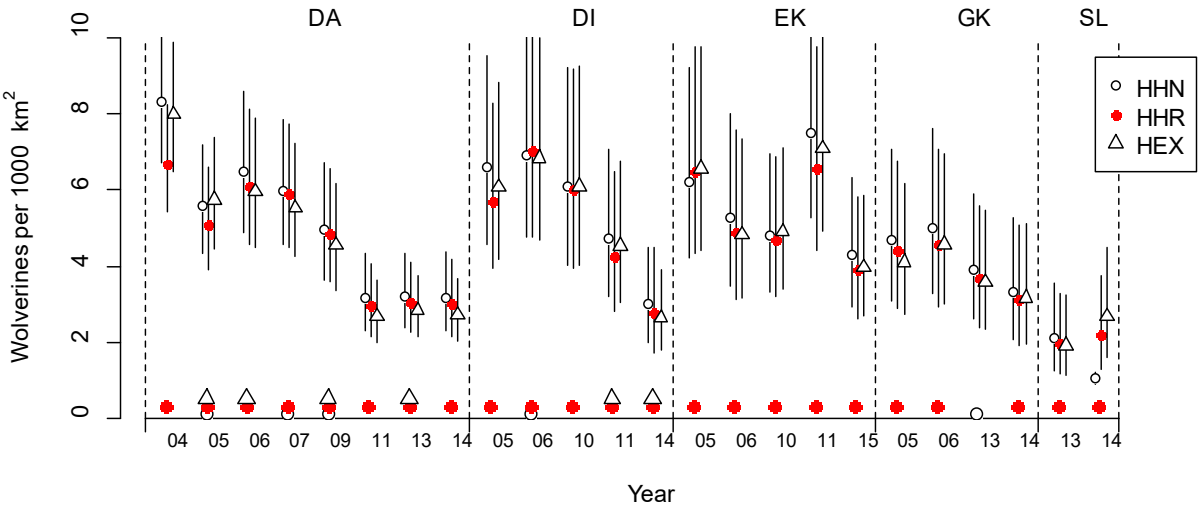

Figure 4.1. Comparison of site-specific estimates of population density from models fitting different detection functions HHN hazard half-normal, HHR hazard hazard-rate, HEX hazard exponential. 95% confidence intervals. Dots at bottom show the model with minimum AIC and any other(s) with ΔAIC<2.0.

Variation in density estimates among detection functions was mostly minor (Figure 4.1). The hazard-rate model was almost uniformly preferred.

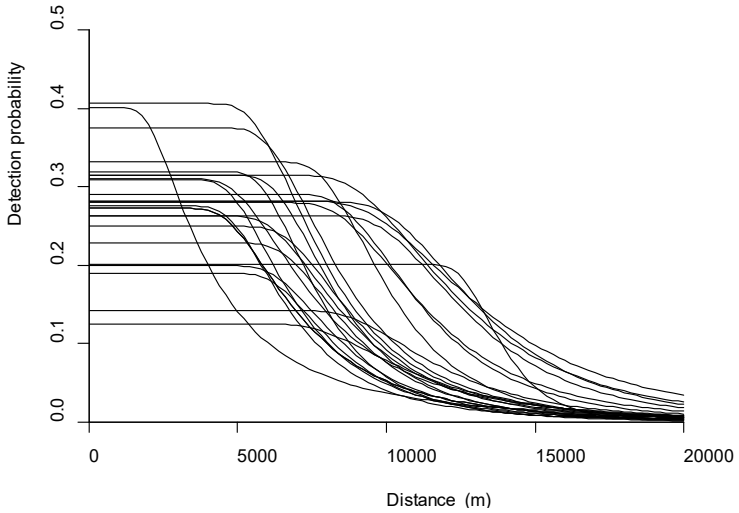

Figure 4.2. Hazard-rate detection functions fitted to the 24 site x year datasets.

Although the fitted functions showed some variation in the extremes, most showed a strong drop off in detection probability between 5 km and 10 km from the activity center (Figure

4.2). Estimates of the shape parameter z were also tightly clustered (interquartile range 4.18–4.92, median 4.56).

Learned (Behavioural) Responses

A case can be made for a site-specific learned response as the favoured model, but the effect on density estimates is negligible in all cases (Figure 4.3).

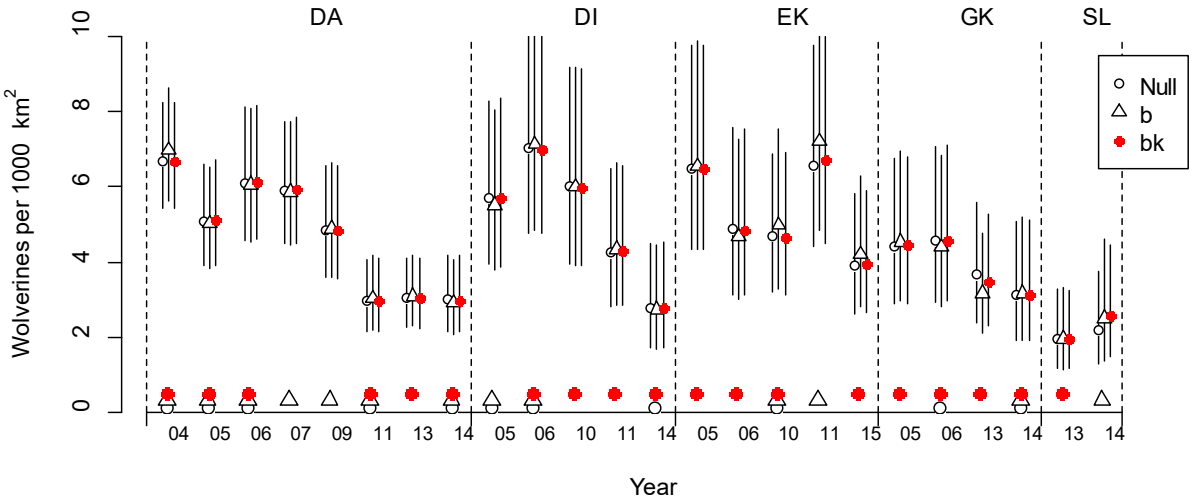

Figure 4.3. Wolverine density estimated from hazard-rate SECR model with no learned response (Null), a persistent general learned response (b), or a site-specific learned response (bk). 95% confidence intervals. Dots below show the model with minimum AIC and any other(s) with ΔAIC<2.0.

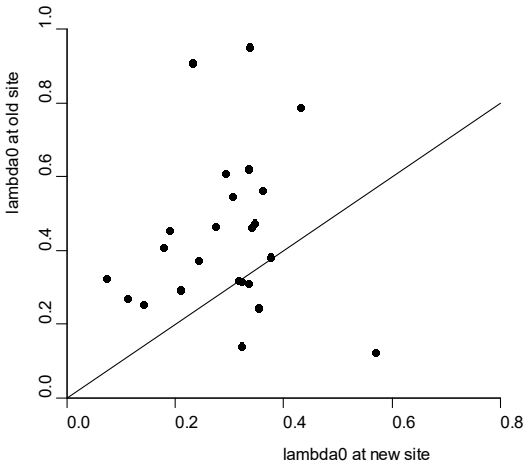

Figure 4.4. Direction of site-specific learned response (bk). 'New' sites were those not yet visited by the animal in question. The estimated effect was usually positive (points lie above line y = x). The extreme point on the x axis is for GK in 2013

Within-year Temporal Variation in Detection Parameters

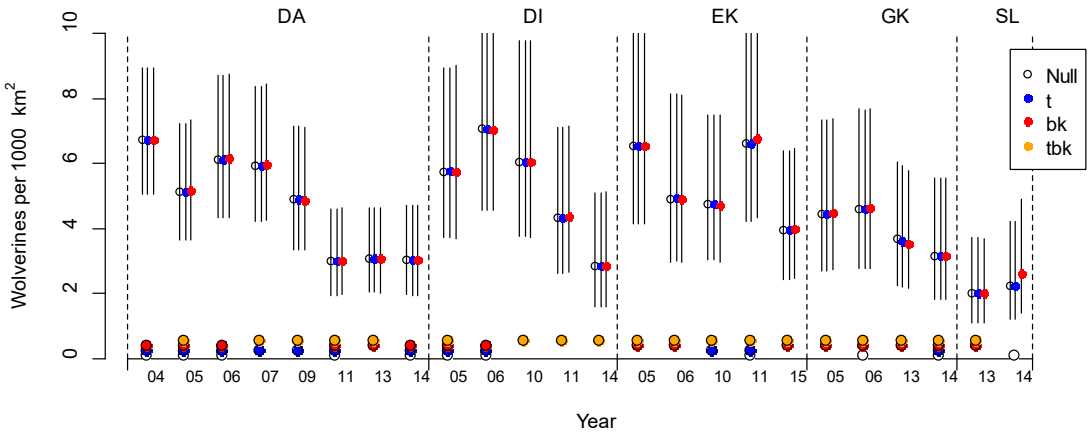

Figure 4.5. Comparison of site-specific estimates of population density from models with temporal variation in detection probability. Hazard-rate detection function and 95% confidence intervals. Dots at bottom show the model with minimum AIC and any other(s) with ΔAIC<2.0.

Although there was support for a temporal effect on detection in some years (e.g. 2007 and 2009 at DA) the effect on density estimates was negligible. It is possible that temporal effects were due to variation in the number of days between post checks, for which we did not control[11].

Sex Differences in Detection

The SECR 'hybrid mixture' model (Efford 2017a) was fitted to each site x year dataset using the covariate 'Sex' to define mixtures. The hazard-rate function was used.

[11] This can be done via the 'usage' attribute in secr (cf Efford, Borchers and Mowat 2013).

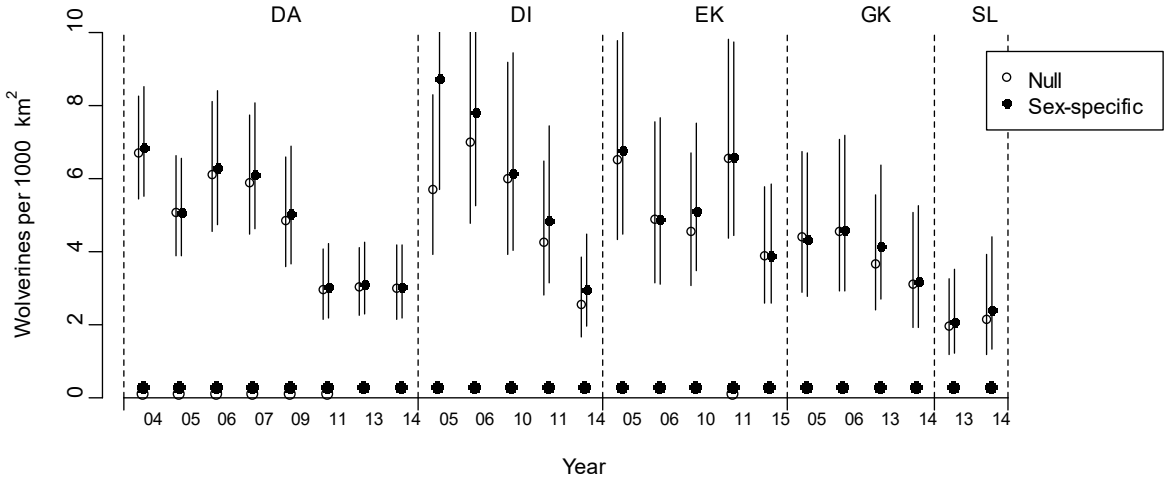

Figure 4.6. Density of both sexes estimated from null detection model (open circles) and a sex-specific detection model (filled circles). The sex-specific model always had lower AIC, although in seven cases the null model was nearly as good (ΔAIC <2) as shown.

Variation Among Sites and Between Years

Density and scale of detection are expected to vary inversely, and the coefficient $k = \sigma\sqrt{D}$ often falls in the range 0.4–0.8 for carnivores (Efford et al. 2016; unpubl. results).

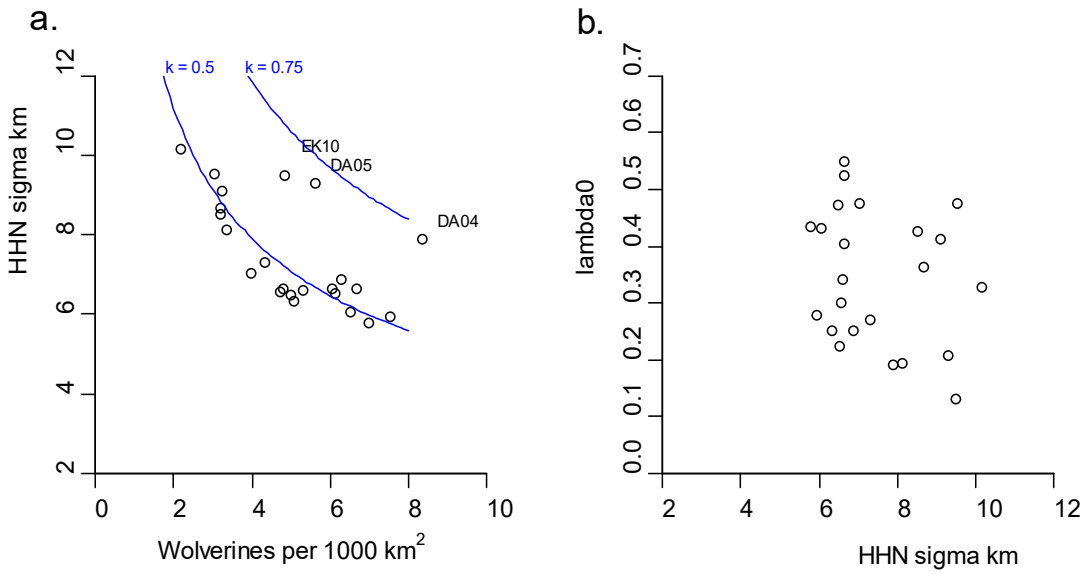

Figure 4.7. Relationships among SECR parameters estimated for each site x year wolverine dataset. For comparison with other studies, we estimate σ for a half-normal detection function.

The relationship in Figure 4.7 suggests that as wolverine density declined the relative home range size as indexed by the scale of detection increased.

APPENDIX 5. LONG-DISTANCE WITHIN-YEAR MOVEMENTS

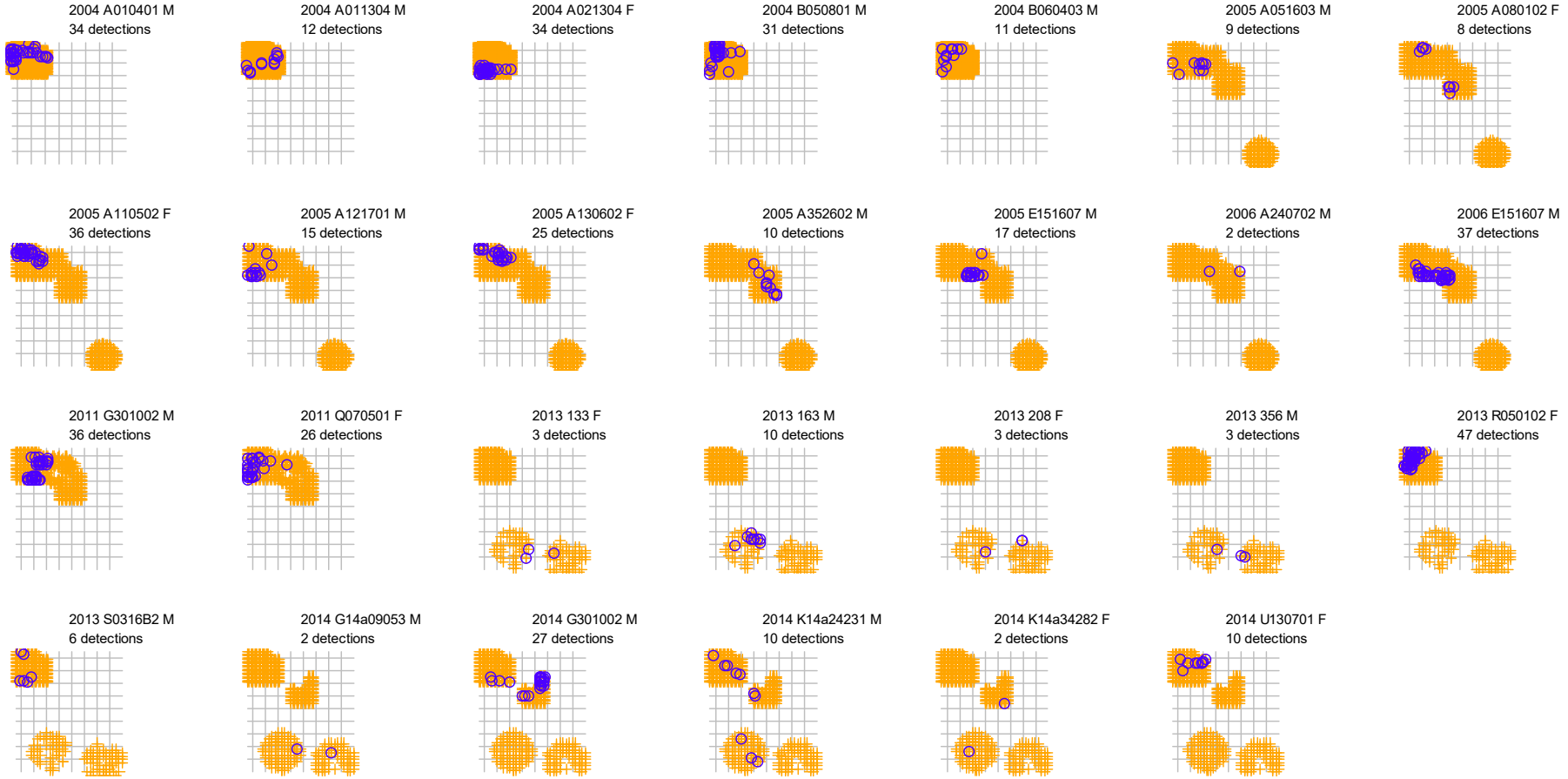

Figure 5.1. Detection locations (blue dots) of individual wolverines whose detections within one season spanned at least 40 km. Grid lines at 20 km spacing. Sex as shown.

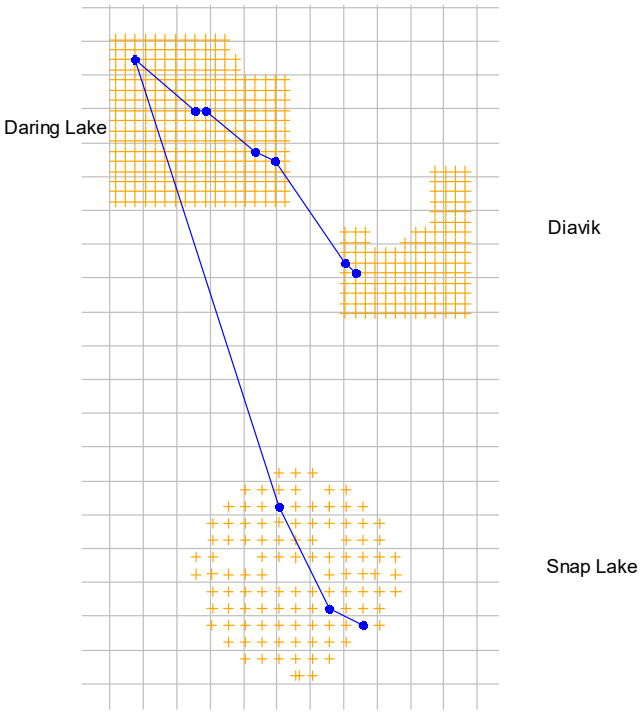

Figure 5.2. Minimum route of male wolverine K14a24231 during sampling in April–May 2014 (total length 276.9 km). 10 km grid squares. The strict sequence in which posts were visited within each sampling interval is not known, so posts are joined here to give the minimum-length total path consistent with the dates of sampling.

APPENDIX 6. HABITAT MASKS

A buffer radius of 40 km was used throughout the analyses in the main text. This was initially computed as five times the half-normal σ-hat from pilot analyses. In view of the high frequency of long-distance movements (Appendix 5), and the choice of a long-tailed (hazard-rate) detection function to accommodate them (Appendix 4) we here check the effect on estimates of ignoring animals centered beyond 40 km.

We performed two checks using the hazard-rate detection function without additional variation (no temporal or learned responses, no sex variation). A pixel size of 3 km x 3 km was used.

Firstly, we predicted the effect of increasing buffer width on site- and year-specific density estimates from the 40-km buffer using the 'esa.plot' function of secr (Efford 2018a).

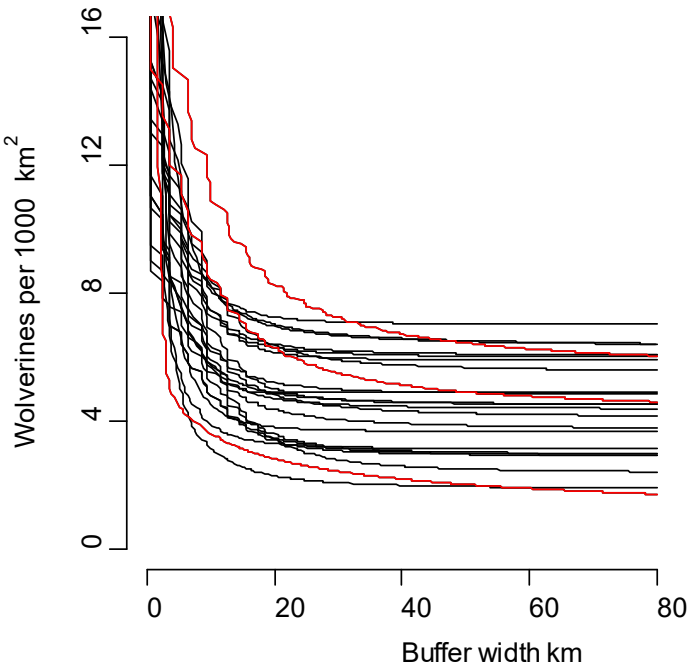

Figure 6.1. Predicted effect of buffer width on density estimates from hazard-rate detection model. Each curve relates to a particular year and site. Most curves become nearly horizontal by the 40 km mark, indicating robustness to further increase in buffer width. Some, particularly the curves in red for DA in 2004 and 2005 and SL in 2014, are still declining at that point.

Secondly, we re-fitted all the site- and year-specific models using a wider (50 km) buffer. This is a more rigorous test because the preceding predictions assume that changing the buffer width does not alter the estimates of the detection parameters (λ_0, σ and z).

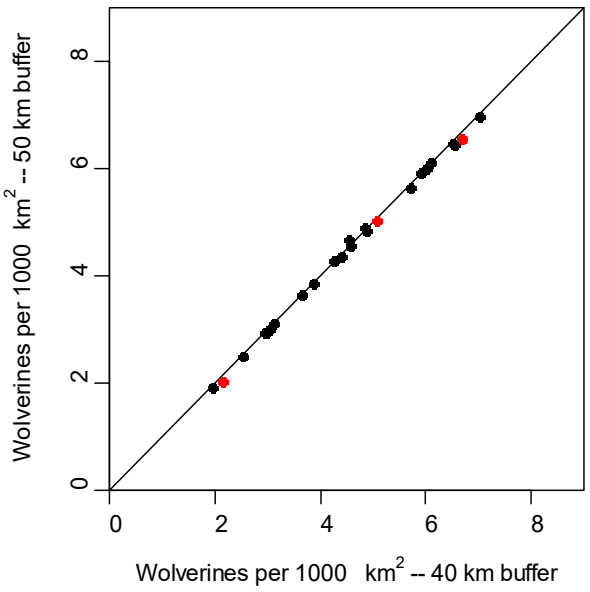

Figure 6.2. Effect of increasing buffer width from 40 km to 50 km on estimates of wolverine density. Each point represents one year and site. No effect is apparent. Points for DA2004, DA2005 and SL2014 shown in red.

We conclude that the chosen buffer width was adequate.

Pixel size is a compromise between computation time (which increases with the number of pixels) and accuracy. Estimates did not change noticeably when we used a smaller pixel size, indicating that a 3 km pixel size is below the threshold at which accuracy becomes an issue (Efford 2017b).

Table 6.1. Area (1,000 km^2) of habitat masks used for site- and year-specific SECR analyses.

		Year										
Site		2004	2005	2006	2007	2008	2009	2010	2011	2012	2013	2014	2015
Daring Lake	DA	15.31	15.02	15.02	15.02	.	15.02	.	15.02	.	15.02	15.02	.
Diavik	DI	.	12.04	12.04	.	.	.	12.04	12.04	.	.	12.04	.
Ekati	EK	.	12.09	12.33	.	.	.	12.93	12.82	.	.	.	12.93
Gahcho Kué	GK	.	11.98	11.98	.	.	.	.	.	.	14.55	14.97	.
Snap Lake	SL	.	.	.	.	.	.	.	.	.	14.30	15.07	.
Northern	DA+DI+EK	.	23.65	23.51	.	.	.	16.71	23.89	.	.	23.01	.

APPENDIX 7. SECR ANALYSES WITH SPATIALLY STRATIFIED DENSITY

We would like separate estimates of the density and trend of the wolverine populations associated with each grid. However, the populations at risk of detection on the DA, EK and DI grids overlap substantially owing to the mobility of wolverines. The machinery of SECR in principle allows for a density model to be stratified into zones associated with each grid, and this was our plan. We considered two stratifications: one in which each stratum was tightly associated with a particular grid except for a pooled outer stratum, and one in which pixels in the outer stratum were assigned to the nearest grid (main text Figure 3). The tighter stratification assigns a small fraction of the wider (mask) population to particular grids (Table 7.1).

Table 7.1. Areas of proposed wolverine population strata (km^2). Percentages in parentheses.

	DA	EK	DI	GK	SL	OU	Total
Stratum	3375	2151	1836	3834	3780	33120	48096
	(7.0)	(4.5)	(3.8)	(8.0)	(7.9)	(68.9)	(100.0)
Wide stratum	10818	5112	6975	13140	12051	––	48096
	(22.5)	(10.6)	(14.5)	(27.3)	(25.1)	––	(100.0)

APPENDIX 8. CAPTURE–RECAPTURE ANALYSIS OF POPULATION TREND

We measure trend as the multiplier lambda (λ) by which density changes from year to year: λ>1.0 represents an increase and λ<1.0 represents a decrease. This factor is also called the finite rate of population increase; λ may be estimated annually, or as a persistent trend across multiple years.

Trend estimates may be derived from a chain of closed-population SECR estimates of density. The fact that some of the same individuals appear in successive years is ignored (each annual population is treated as an independent sample). Non-independence can cause λ to be estimated with spurious precision (M. Efford unpubl.), but the method is robust to changes in the extent of the study area.

A more comprehensive approach that allows for the in situ survival of some animals (and hence incorporates non-independence) is to model turnover (mortality and recruitment) along the chain of samples in an "open population" model. Early approaches relied on the temporal symmetry of capture histories: just as apparent survival φ may be estimated from recaptures forwards in time, a seniority parameter ϒ may be estimated from the same arithmetic applied to reversed capture histories, and λ at time *t* may be estimated as the ratio φ_t / Υ_{t+1} (Pradel 1996). This is one of several possible ways to parameterize recruitment and turnover in open-population models of the Jolly–Seber or Schwarz–Arnason type. In some formulations, including the one we used, λ appears directly as a parameter in the model. Alternatively, recruitment may be represented in the model by the per capita rate *f*; λ is then calculated as the derived parameter $\lambda_t = f_t + \varphi_t$. The various turnover parameters (φ, ϒ, f, λ) may be estimated while conditioning on detection (i.e., without modeling the number of all-zero histories to estimate population size). Relationships among the various formulations were reviewed by Schwarz and Arnason (2017; see also Franklin 2001 and Link and Barker 2006).

Non-spatial open-population estimators for λ work well as long as the extent of sampling (and hence of the study population) does not change, and there is no behavioural response to capture (e.g. Hines and Nichols 2002).

Open-population SECR models have the potential to combine the strengths of the preceding methods (closed-population SECR and open-population non-spatial CR). They also potentially separate emigration and mortality (Ergon and Gardner 2014, Schaub and Royle 2014). Custom open-population SECR models have been used in several studies (Gardner et al. 2010, Chandler and Clark 2014). We have developed general software for open-population SECR analysis (Efford 2018b). However, for the wolverine analysis we compared trend estimates from closed-population SECR and open-population non-spatial CR; open-population SECR analyses are not presented.

LITERATURE CITED

Barrueto, M., A. Forshner, J. Whittington, A.P. Clevenger and M. Musiani. 2022. Protection status, human disturbance, snow cover and trapping drive density of a declining wolverine population in the Canadian Rocky Mountains. *Scientific Reports* 12:17,412.

Bivand, R., T. Keitt and B. Rowlingson. 2017. rgdal: Bindings for the 'Geospatial' Data Abstraction Library. R package version 1.2-16. https://CRAN.R-project.org/package=rgdal

Borchers, D.L. and M.G. Efford. 2008. Spatially explicit maximum likelihood methods for capture–recapture studies. *Biometrics* 64: 377–385.

Borchers, D.L. and M.G. Efford. 2007. Supplements to Biometrics paper. www.otago.ac.nz/density/pdfs/Supplement to Borchers and Efford v2.pdf.

Boulanger, J. and R. Mulders. 2013a. Analysis of wolverine DNA mark-recapture sampling at Daring Lake, Diavik, and Ekati, Northwest Territories from 2005 to 2011. Environment and Natural Resources, Government of the Northwest Territories.

Boulanger, J. and R. Mulders. 2013b. Analysis of wolverine DNA mark-recapture sampling at Daring Lake, from 2004 to 2011. Environment and Natural Resources, Government of the Northwest Territories.

Buckland, S.T., D.R. Anderson, K.P. Burnham, J.L. Laake, D.L. Borchers and L. Thomas. 2001. Introduction to Distance Sampling. Oxford University Press, Oxford.

Chandler, R.B. and J.D. Clark. 2014. Spatially explicit integrated population models. Methods in Ecology and Evolution 5:1,351–1,360.

Efford, M. 2004. Density estimation in live-trapping studies. Oikos 106:598-610.

Efford, M.G. 2012. DENSITY 5.0: software for spatially explicit capture–recapture. Department of Mathematics and Statistics, University of Otago, Dunedin, New Zealand. www.otago.ac.nz/density

Efford, M.G. 2017a. Finite mixture models in secr 3.0. www.otago.ac.nz/density/pdfs/secr-finitemixtures.pdf.

Efford, M.G. 2017b. Habitat masks in the package secr. www.otago.ac.nz/density/pdfs/secr-habitatmasks.pdf.

Efford, M.G. 2017c. Multi-session models in secr 3.0. www.otago.ac.nz/density/pdfs/secr-multisession.pdf.

Efford, M.G. 2018a. secr: Spatially explicit capture-recapture models. R package version 3.1.4. https://CRAN.R-project.org/package=secr.

Efford, M.G. 2018b. openCR: Open population capture-recapture models. R package version 1.1.1, https://CRAN.R-project.org/package=openCR/.

Efford, M.G., D.L. Borchers and A.E. Byrom. 2009. Density estimation by spatially explicit capture-recapture: likelihood-based methods. In: D.L. Thomson, E.G. Cooch and M.J. Conroy (eds.) Modeling Demographic Processes in Marked Populations. Springer, NY. Pp. 255–269.

Efford, M.G., D.L. Borchers and G. Mowat. 2013. Varying effort in capture–recapture studies. Methods in Ecology and Evolution 4: 629–636.

Efford, M.G., D.K. Dawson, Y.V. Jhala and Q. Qureshi. 2016. Density-dependent home range size revealed by spatially explicit capture–recapture. Ecography 39:676–688.

Efford, M.G. and R.M. Fewster. 2013. Estimating population size by spatially explicit capture–recapture. Oikos 122: 918–928.

Efford, M. and J. Boulanger. 2019. Fast evaluation of study designs for spatially explicit capture recapture. Methods in Ecology and Evolution 10:1,529–1,535.

Efford, M.G. and M.R. Schofield. 2020. A spatial open-population capture-recapture model. Biometrics 76: 392–402.

Ergon, T. and B. Gardner. 2014. Separating mortality and emigration: modelling space use, dispersal and survival with robust-design spatial capture–recapture data. Methods in Ecology and Evolution 5: 1,327–1,336.

Ergon, T. and B. Gardner. 2014. Separating mortality and emigration: modelling space use, dispersal and survival with robust-design spatial capture–recapture data. Methods in Ecology and Evolution 5: 1,327–1,336.

Gardner, B., J. Reppucci, M. Lucherini and J.A. Royle. 2010. Spatially explicit inference for open populations: estimating demographic parameters from camera-trap studies Ecology 91: 3,376–3,383.

Hines, J.E. and J.D. Nichols. 2002. Investigations of potential bias in the estimation of λ using Pradel's (1996) model for capture- recapture data. Journal of Applied Statistics 29: 573–587.

Franklin, A.B. 2001. Exploring ecological relationships in survival and estimating rates of population change using Program MARK. Pp. 350–356 in R. Field, R.J. Warren, H. Okarma and P.R. Sievert (eds) Wildlife, land, and people: priorities for the 21st century. The Wildlife Society.

Gardner, B., J. Reppucci, M. Lucherini and J.A. Royle. 2010. Spatially explicit inference for open populations: estimating demographic parameters from camera-trap studies Ecology 91: 3,376–3,383.

Hines, J.E. and J.D. Nichols. 2002. Investigations of potential bias in the estimation of λ using Pradel's (1996) model for capture- recapture data. Journal of Applied Statistics 29: 573–587.

Link, W.A. and R.J. Barker. 2006. Modeling association among demographic parameters in analysis of open population capture–recapture data. Biometrics 61: 46–54.

Milleret, C., S. Dey, P. Dupont, H. Brøseth, D. Turek, P. de Valpine, R. Bischof. 2022. Estimating spatially variable and density-dependent survival using open-population spatial capture–recapture models. Ecology e3934, 1–11. https://doi.org/10.1002/ecy.3934

Mulders, R., J. Boulanger and D. Paetkau. 2007. Estimation of population size for wolverines *Gulo gulo* at Daring Lake, Northwest Territories, using DNA based mark-recapture methods. Wildlife Biology 13, Supplement 2: 32–51.

Pledger, S., K.H. Pollock and J.L. Norris. 2010. Open capture–recapture models with heterogeneity: II. Jolly–Seber model. Biometrics 66: 883–890.

Paetkau, D. 2003. An empirical exploration of data quality in DNA-based population inventories. Molecular Ecology 12: 1,375–1,387.

Pollock, K.H. 1982. A capture–recapture design robust to unequal probability of capture. Journal of Wildlife Management 46: 752–757.

Pradel, R. 1996 Utilization of capture-mark-recapture for the study of recruitment and population growth rate. Biometrics 52: 703–709.

R Core Team. 2017. R: A language and environment for statistical computing. R Foundation for Statistical Computing, Vienna, Austria. www.R-project.org/

Royle, J.A., R.B. Chandler, R. Sollmann and B. Gardner. 2014. Spatial Capture–Recapture. Academic Press, Waltham, MA.

Schaub, M. and J.A. Royle. 2014. Estimating true instead of apparent survival using spatial Cormack–Jolly–Seber models. Methods in Ecology and Evolution 5: 1,316–1,326.

Schwarz, C.J. and A.N. Arnason. 1996. A general methodology for the analysis of capture–recapture experiments in open populations. Biometrics 52: 860–873.

Schwarz, C.J. and A.N. Arnason. 2017. Jolly-Seber models in MARK. Chap. 12 in Cooch and White (eds.) Program MARK: A Gentle Introduction. 17th edition. www.phidot.org/software/mark/docs/book/.